Mon. Not. R. Astron. Soc. **000**, 000–000 (0000) Printed 14 February 2017 (MN LATEX style file v2.2)

Galaxy Zoo: The interplay of quenching mechanisms in the group environment

R. J. Smethurst,[1,2] C. J. Lintott,[1] S. P. Bamford,[2] R. Hart,[2]
S. Kruk,[1] K. L. Masters,[3] R. C. Nichol,[3] and the Galaxy Zoo team ⋆
[1] *Oxford Astrophysics, Department of Physics, University of Oxford, Denys Wilkinson Building, Keble Road, Oxford, OX1 3RH, UK*
[2] *School of Physics and Astronomy, The University of Nottingham, University Park, Nottingham, NG7 2RD, UK*
[3] *Institute of Cosmology and Gravitation, University of Portsmouth, Dennis Sciama Building, Barnaby Road, Portsmouth, PO1 3FX, UK*

14 February 2017

ABSTRACT
Does the environment of a galaxy directly influence the quenching history of a galaxy? Here we construct a sample of group and field galaxies with morphological classifications from Galaxy Zoo 2 and use Bayesian inference to determine the quenching time and rate that describes a simple exponentially declining SFH for a given galaxy from its optical and NUV colours. We investigate how detailed morphological structures, such as bar and bulge fractions, change with projected group radius and correlate this with trends in the SFHs in a mass independent sample. We find that the time since quenching and the rate of quenching do not correlate with the velocity of a satellite through the group but are correlated with the group potential. This quenching occurs within an average quenching timescale of ~ 2.5 Gyr from star forming to complete quiescence, during an average infall time (from $\sim 10R_{200}$ to $0.1R_{200}$) of ~ 2.4 Gyr. This suggests that the environment does play a direct role in galaxy quenching through a quenching mechanism which is correlated with the group potential, such as harassment, interactions and starvation. Environmental quenching mechanisms which are correlated with satellite velocity, such as ram pressure stripping, are therefore not the main cause of quenching in the group environment. Instead an interplay of mergers, mass & morphological quenching and environment driven quenching mechanisms dependent on the group potential drive the evolution of group galaxies.

Key words: galaxies – environment, galaxies – photometry, galaxies – statistics, galaxies – morphology

1 INTRODUCTION

Galaxies are often found clustered together in groups (Zwicky 1938, 1952; Abell 1958), all sharing one large dark matter halo (groups with 100 or more galaxies are referred to as clusters; Bower & Balogh 2004). Conversely some galaxies are found isolated from others in less dense environments (often referred to as the field), either because they are fossil groups (where all members have eventually merged; Ponman et al. 1994; Jones et al. 2000, 2003) or have truly been isolated for their entire lifetimes. This environmental density is found to be correlated with morphology (Dressler 1980; Smail et al. 1997; Poggianti et al. 1999; Postman et al. 2005; Bamford et al. 2009), colour (Butcher & Oemler 1978; Pimbblet et al. 2002), quenched galaxy fraction (Kauffmann et al. 2003; Baldry et al. 2006; Peng et al. 2012; Darvish et al. 2016) and SFR (Gómez et al. 2003). Star forming disc galaxies tend to be located in low-density environments with quiescent early-type galaxies in more dense environments. This suggests that the environment may drive a galaxy's transition from star forming in the blue cloud to the quiescent red sequence through quenching of star formation.

Although these correlations were originally interpreted as indicating causation, recent evidence from simulations suggests that quenching mechanisms driven by the environment may not be dominant in the galaxy lifecycle (Kimm et al. 2009, 2011; Hirschmann et al. 2014; Wang et al. 2014; Phillips et al. 2015; Emerick et al. 2016; Fillingham et al. 2016). Perhaps, instead, the correlation of increased quenched galaxy fractions with environment density is due to a superposition of other possible quenching mechanisms each of which depend on more local factors than the broader environment properties.

⋆ This investigation has been made possible by the participation of over 350,000 users in the Galaxy Zoo project. Their contributions are acknowledged at `http://authors.galaxyzoo.org`

In order to isolate the cause of the density-morphology and density-SFR correlations, we need to observe how morphology and galaxy quenching timescales change in dense environments with different properties in comparison to the field. Here, we consider the group environment, as this is a more typical environment for a galaxy than the relatively rare rich cluster environment (Carlberg 2004). We construct a sample of both group and field galaxies and use a Bayesian inference method to determine the quenching time and rate describing a simple exponentially declining SFH for a galaxy given its optical and NUV colours. From these inferred SFHs we aim to constrain the possible mechanisms at work in the group environment. We aim to determine the following: (i) How does the environment influence the detailed morphological structures of a galaxy? (ii) Is quenching which is directly caused by the environment occurring in galaxy groups? However, dense environments are messy with many possible mechanisms at work, whose effects are difficult to disentangle.

There are many mechanisms which have been suggested to cause quenching. They are often referred to as either internal mechanisms (caused by the galaxy's 'nature') or external mechanisms (caused by the way the galaxy is 'nurtured'). The properties of a galaxy and its environment are often thought to control which mechanisms will affect a galaxy throughout its lifetime and subsequently affect the morphology. Here we introduce the basic principles of possible quenching mechanisms; we provide a more thorough discussion in Section 5. Readers who are well versed in quenching mechanisms may wish to skip to Section 2 wherein we describe the data sources and samples.

1.1 Internal Quenching Mechanisms

1.1.1 Mass quenching

Mass quenching is defined by Peng et al. (2010, 2012) as any quenching mechanism acting independently of a galaxy's environment, but not of its mass. However, there is still much debate over the exact mechanism which is the cause of such a quench. Darvish et al. (2016) suggest that non-AGN driven feedback mechanisms (for example supernova feedback) are responsible for the correlation observed between the mass quenching efficiency and SFR in Peng et al. (2010). However, Gabor & Davé (2015) suggest that this is driven by "halo quenching processes" whereby the inflow of cool gas from the galaxy halo is either cut off or hindered from cooling at $M_{\rm halo} > 10^{12}$ $M_{\odot}$ (Birnboim & Dekel 2003; Dekel & Birnboim 2006). If this happens, a galaxy uses up the rest of its available gas for star formation via the Kennicutt-Schmidt law (Schmidt 1959; Kennicutt 1998) and consequently grows in mass.

In this work, we refer to mass quenching as a cut off of gas inflow, resulting in a gradual consumption of gas in star formation. This definition of mass quenching is thought to be a dominant mechanism for isolated galaxies in the field (Kormendy & Kennicutt 2004). However, it is also thought that as a galaxy infalls in to a group or cluster over long timescales, gas reservoirs can also be depleted via a mass quenching process (Peng et al. 2012).

We investigate this possible quenching mechanism in this study by studying the dependency of the inferred quenching parameters with stellar mass for satellite, central and field galaxies.

1.1.2 Morphological quenching

Morphological quenching is the process by which the internal structure of a galaxy can have a negative impact on its own SFR. This can happen in one of two ways, either by preventing star formation from occurring or by increasing the rate of consumption of gas for star formation. The former is thought to be caused by bulges (Bluck et al. 2014) whereby the large gravitational potential of the bulge prevents the disc from collapsing and forming stars (Fang et al. 2013).

The latter mechanism is thought to occur in galaxies hosting bars; the bar funnels gas to the centre of the galaxy (Athanassoula 1992a) where gas is exhausted by star formation effectively quenching the galaxy (Zurita et al. 2004; Sheth et al. 2005).

We investigate this possible quenching mechanism in this study by studying the dependency of the bar and bulge fractions of satellite galaxies in comparison to the field.

1.1.3 AGN feedback as a quenching mechanism

There are tight correlations between properties of galaxies, such as the bulge mass, total stellar mass & stellar velocity dispersion, and black hole mass (Magorrian et al. 1998; Marconi & Hunt 2003; Häring & Rix 2004). This implies a co-evolution between the black hole and its host galaxy therefore suggesting that changes in the SFR and structure of a galaxy could also be tied to black hole activity. This is thought to occur via AGN feedback where the output of energetic material and radiation from the black hole is thought to either heat or expel the gas needed for SF in a galaxy, causing a quench.

AGN feedback was first suggested as a mechanism for regulating star formation due to the results of simulations wherein galaxies could grow to unrealistic stellar masses (Silk & Rees 1998; Bower et al. 2006; Croton et al. 2006; Somerville et al. 2008). Without a prescription for the effects of AGN feedback, the shape of the galaxy luminosity function could therefore not be matched at the high luminosity end (Baugh et al. 1998, 2005; Kauffmann et al. 1999a,b; Somerville et al. 2001; Kitzbichler & White 2006).

Indirect observational evidence has been found for both positive and negative feedback in various systems (see the comprehensive review from Fabian 2012). The strongest being the indirect evidence that the largest AGN fraction is found in the green valley (Cowie & Barger 2008; Hickox et al. 2009; Schawinski et al. 2010), suggesting a link between AGN activity and the process which moves a galaxy from the blue cloud to the red sequence. Recent statistical evidence from Smethurst et al. (2016) has shown the dominance of rapid, recent quenching within a population of Type 2 AGN host galaxies, suggesting that AGN feedback is indeed an important evolutionary mechanism.

We do not directly investigate the presence of AGN in the group environment due to constraints from low number statistics, however we discuss the possible role of AGN feedback in the context of the results presented in this study in Section 5.5.

1.2 External Quenching Mechanisms

1.2.1 Mergers as a quenching mechanism

Major mergers have been intrinsically linked to the formation of early-type galaxies since Toomre & Toomre (1972) showed this was possible with a simulation of the merger of two equal mass disc galaxies. The hypothesis is as follows: when two galaxies merge, the influx of cold gas funnelled by the forces in the interaction often results in energetic starbursts (Mihos & Hernquist 1994, 1996; Hopkins et al. 2006a, 2008b,a; Snyder et al. 2011; Hayward et al. 2014; Sparre & Springel 2016), which can exhaust the gas required for star formation, effectively quenching the post-merger remnant. This remnant galaxy will also have formed a dynamically hot bulge through the dissipation of angular momentum in the merger (Toomre 1977; Walker et al. 1996; Kormendy & Kennicutt 2004; Hopkins et al. 2012; Martig et al. 2012). The mass ratio of the two galaxies merging is thought to affect the size of the bulge that is formed in the remnant (Cox et al. 2008; Hopkins et al. 2009; Tonini et al. 2016), with the most massive major mergers with a 1:1 mass ratio producing fully elliptical galaxies (Toomre & Toomre 1972; Barnes & Hernquist 1996; Mihos & Hernquist 1996; Kauffmann 1996; Pontzen et al. 2016). However, recent simulations of the merger of two disc galaxies with a 1:1 mass ratio have shown that the a disc remnant galaxy can be produced (Hopkins et al. 2009; Pontzen et al. 2016; Sparre & Springel 2016).

Such a scenario is also intrinsically linked to the triggering of an AGN due to the influx of gas in the merger which can fuel the black hole accretion (Sanders et al. 1988; Di Matteo et al. 2005; Hopkins & Hernquist 2009; Treister et al. 2012). Simulations of mergers with AGN have led many to believe that a merger which triggers both a starburst and an AGN can quench a galaxy in extremely rapid timescales (Springel et al. 2005; Bell et al. 2006). Recent simulations have also suggested that feedback from the triggered AGN (see Section 1.1.3) is necessary to fully remove (or heat) all the available gas, otherwise the SFR will recover back to the SFS post-merger (Athanassoula et al. 2016; Pontzen et al. 2016; Sparre & Springel 2016).

Mergers also have a clear environmental dependence, as they are more likely to occur in denser environments (at least until the velocity dispersion of a cluster becomes so large as to suppress mergers due to increased interaction velocities between galaxies). However, their effects must be separated from those quenching mechanisms driven solely by the properties of the galaxy environment. We investigate mergers as a possible quenching mechanism in this study by studying the dependency of the inferred quenching parameters with the number of galaxies in a group .

1.2.2 Environment driven quenching

The proposed quenching mechanisms under the umbrella of environmental quenching are numerous and varied. Together with the typical gravitational galaxy-galaxy interactions (Moore et al. 1996) which are expected to be more frequent in a dense environment, environmental quenching also includes hydrodynamic interactions occurring between the cold interstellar medium (ISM) of the in-falling galaxy and the hot intergalactic medium (IGM) of the group or cluster. Such hydrodynamic interactions include ram pressure stripping (Gunn & Gott 1972), viscous stripping (Nulsen 1982), and thermal evaporation (a rapid rise in temperature of the ISM due to contact with the IGM; Cowie & Songaila 1977). Another such process is starvation (also called strangulation; Larson et al. 1980) which can remove the outer galaxy halo, thus cutting off the star formation gas supply to a galaxy. Preprocessing occurs when all of the above mechanisms take place in a group of galaxies which then merges with a larger group or cluster (Dressler 2004).

The most likely (and therefore the most studied) candidate mechanism for the cause of the environmental density-morphology and SFR relations is ram pressure stripping (RPS; Abadi et al. 1999; Poggianti et al. 1999). However, there has been mounting evidence that RPS can only strip a galaxy of $40-60\%$ of its gas supply (Fillingham et al. 2016) and so may not be as effective a quenching mechanism as first thought (Emerick et al. 2016). Therefore investigations of other environmentally driven quenching mechanisms, such as strangulation (Peng et al. 2015; Hahn et al. 2016; Maier et al. 2016; Paccagnella et al. 2016; Roberts et al. 2016; van de Voort et al. 2016) and harassment (high speed galaxy 'fly-by' gravitational interactions Bialas et al. 2015; Smith et al. 2015) are having a recent resurgence.

We investigate the environment as a possible driver of quenching in this study by studying the dependency of the inferred quenching parameters with halo mass, satellite : central mass ratio, the relative velocity of satellites and the stellar velocity dispersions of group galaxies in comparison to the field.

This paper proceeds as follows. In Section 2 we describe our data sources and group galaxy sample. We show the results of an investigation into the environmental dependence of the detailed morphological structure of group galaxies in Section 3. We describe our Bayesian inference method for determining the quenching histories of group galaxies and present the results of this method in Section 4. We then discuss the possible quenching mechanisms that could be responsible for our results and how they fit into the bigger picture of quenching in Section 5. We summarise our findings in Section 6. The zero points of all magnitudes are in the AB system. Where necessary, we adopt the WMAP Seven-Year Cosmology (Jarosik et al. 2011) with $(\Omega_m,\ \Omega_\Lambda,\ h) = (0.26, 0.73, 0.71)$.

2 DATA AND METHODS

2.1 Data Sources

In this investigation we use visual classifications of galaxy morphologies from the Galaxy Zoo 2[1] (GZ2) citizen science project (Lintott et al. 2009; Willett et al. 2013), which obtains multiple independent classifications for each optical image. The full question tree for an image is shown in Figure 1 of Willett et al. The GZ2 project used 304, 022 images from the Sloan Digital Sky Survey Data Release 7 (SDSS; York et al. 2000; Abazajian et al. 2009) all classified by *at*

[1] `http://zoo2.galaxyzoo.org/`

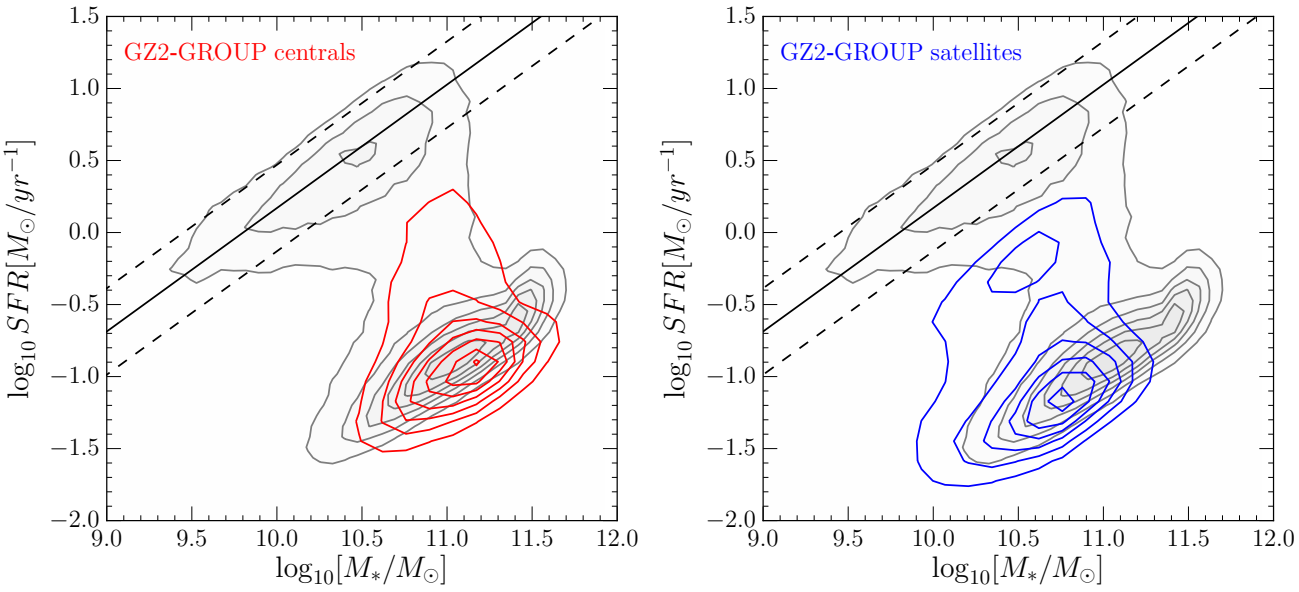

Figure 1. The stellar mass-SFR plane showing central (left; red contours) and satellite (right; blue contours) in the GZ2-GROUP sample. In both panels the entire SDSS sample from the MPA-JHU catalogue is shown by the grey contours. The definition of the SFS from Peng et al. (2010) at $\overline{z} = 0.053$ (solid line, the mean redshift of the GZ2-GROUP sample) with $\pm 1\sigma$ (dashed lines) is shown.

least 17 independent users, with a mean number of classifications of ~ 42. We also utilise the Petrosian magnitude, `petroMag`, values for the u (3,543Å) and r (6,231Å) wavebands provided by the SDSS pipeline for the GZ2 galaxies.

Further to this, we required NUV (2,267Å) photometry from the GALEX survey (Martin et al. 2005), within which $\sim 42\%$ of the GZ2 sample was observed, giving 126,316 galaxies total ($0.01 < z < 0.25$). This will be referred to as the GZ2-GALEX sample. The completeness of this sample is shown in Figure 2 of Smethurst et al. (2015).

Magnitudes are corrected for galactic extinction (Oh et al. 2011) by applying the Cardelli et al. (1989) law, giving a typical correction of $u - r \sim 0.05$. K-corrections are also adopted to $z = 0.0$ and absolute magnitudes obtained from the NYU-VAGC (Blanton et al. 2005; Padmanabhan et al. 2008; Blanton & Roweis 2007), giving a typical $u - r$ correction of ~ 0.15 mag.

2.2 Group Identification

The construction of a robust cluster or group catalogue is a challenge, with many studies attempting this across the SDSS (e.g. Merchán & Zandivarez 2005; Miller et al. 2005; Berlind et al. 2006; Yang et al. 2007; Tago et al. 2008, 2010; Tinker et al. 2011; Muñoz-Cuartas & Müller 2012; Tempel et al. 2014) and other large surveys (Tucker et al. 2000; Merchán & Zandivarez 2002; Eke et al. 2004; Cucciati et al. 2010; Robotham et al. 2011; Knobel et al. 2012). The difficulties arise in removing projection effects, understanding the selection function used, covering large ranges in mass and redshift, and dealing with spectral fibre collisions (see the comprehensive review by Postman 2002 for an in depth discussion).

In this work we use the Berlind et al. (2006) catalogue, which employs a friends-of-friends algorithm to identify group galaxies in the SDSS DR4. This group catalogue was then cross matched with the GZ2-GALEX sample. We limit our sample to $z < 0.1$ to ensure GALEX completeness to the red sequence, as in Wyder et al. 2007; Yesuf et al. 2014, so that we do not introduce any bias in our sample due to the necessity for NUV colours. This results in 10,423 group galaxies with the number of group members, $N_{\rm group} \geqslant 3$. Centrals are identified as the brightest group galaxy in the r-band, with all other galaxies in a group designated as satellites.

The projected group-centric radius, R, of all satellite galaxies from their central galaxies was calculated. In order to compare groups of different sizes, the virial radius is used as a normalisation factor to this projected group-centric radius. Here we use a proxy to the virial radius, R_{200} (see Navarro et al. 1995), the radius within which the group mass overdensity is 200 times the critical density, $\rho_{\rm crit}(z)$, as defined by Finn et al. 2005:

$$200\rho_{\rm crit}(z) = \frac{M_{cl}}{\frac{4}{3}\pi R_{200}^3}, \tag{1}$$

where M_{cl} is the mass of the group. Finn et al. then use the redshift dependence of the critical density and the virial mass to relate the line-of-sight velocity dispersion of the group, σ_x, to the group mass so that R_{200} becomes:

$$R_{200} = 1.73 \left(\frac{\sigma_x}{1000 \text{km s}^{-1}}\right) \cdot \frac{1}{\sqrt{\Omega_\Lambda + \Omega_o(1+z)^3}}\, h_{100}^{-1} \text{ Mpc}. \tag{2}$$

σ_x is provided in the Berlind et al. (2006) catalogue and is calculated as:

$$\sigma_x = \frac{1}{1+\overline{z}} \sqrt{\frac{1}{N_{\rm group} - 1} \sum_{i=1}^{N_{\rm group}} (cz_i - c\overline{z})^2} \tag{3}$$

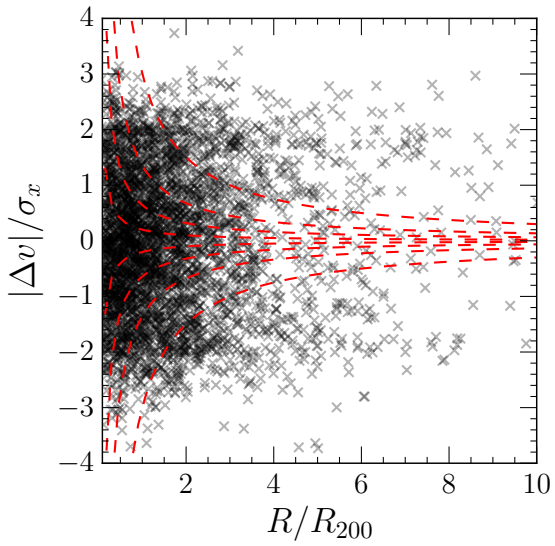

Figure 2. Phase space distribution of satellite galaxies in the GZ2-GROUP sample showing caustics at constant $(\Delta v/\sigma) \times (R/R_{200}) = \{3, 1.35, 0.64, 0.2\}$ as in Noble et al. (2016).

where $\overline{z}$ is the mean redshift of the group and $N_{\rm group}$, the number of galaxies in a group. Since most groups in the sample have low $N_{\rm group}$, using the mean redshift for $z_{\rm group}$, rather than the central galaxy redshift is most appropriate in this case. These calculations resulted in a sample of 2,209 centrals and 8,214 satellites within a projected group-centric radius range of $0.01 < R/R_{200} < 10.0$ and $z < 0.084$ which shall be referred to as the GZ2-BERLIND sample. Note that for a galaxy (central or satellite) to be included in the GZ2-BERLIND sample, the rest of its group does not. However the properties of that group are still retained by the included galaxy.

We obtain SFRs, stellar masses and stellar velocity dispersions of galaxies in the GZ2-BERLIND sample from the MPA-JHU catalogue (Kauffmann et al. 2003; Brinchmann et al. 2004). The measurements of stellar velocity dispersion, σ_*, from the MPA-JHU catalogue are limited by the SDSS instrument dispersion of $\sim$ 69 km s^{-1} (Stoughton et al. 2002). Therefore any σ_* values derived below the instrument dispersion are assumed to be upper limits at 70 km s^{-1}.

In this study we specifically focus on galaxies that are below the star forming sequence (SFS). We select a subsample of the GZ2-BERLIND galaxies that are 1σ below the SFS (as defined by Peng et al. 2010), giving 3,867 satellite and 1,564 central galaxies which will collectively be referred to as the GZ2-GROUP sample (with a median $N_{\rm group} = 8$, mean $N_{\rm group} \sim 26$ and maximum $N_{\rm group} = 311$). These galaxies are shown in the panels of Figure 1 and can be seen to lie below the SFS.

We also show the GZ2-GROUP satellite galaxies on a phase space diagram, shown in Figure 2, with the normalised projected group-centric radius and normalised relative velocity of the satellites to their central. We also over plot caustics at constant $(\Delta v/\sigma) \times (R/R_{200}) = \{3, 1.35, 0.64, 0.2\}$ as in Noble et al. (2016). They define those galaxies with $3 < (\Delta v/\sigma) \times (R/R_{200}) < 1.35$ as infalling satellites, $1.35 < (\Delta v/\sigma) \times (R/R_{200}) < 0.64$ as recently accreted satellites, $0.64 < (\Delta v/\sigma) \times (R/R_{200}) < 0.2$ as intermediate/backsplashing satellites and $0.2 < (\Delta v/\sigma) \times (R/R_{200}) < 0$ as central satellites.

We find that 23% of the GZ2-GROUP satellites lie outside of the outer caustic with $(\Delta v/\sigma) \times (R/R_{200}) > 3$. This is caused by projection effects for one of two possible reasons; either the true radius has been overestimated by the projected radius or the satellite has been misidentified as a member of a group. We chose to retain these galaxies within our sample since we cannot distinguish between these two effects (however we note that removing them does not change our conclusions). This is only an issue for satellites with $R/R_{200} > 1$.

We also consider the projected neighbour density, as defined by Baldry et al. (2006) as $\Sigma_N = N/4\pi d_N^2$, where d_N is the distance to the $N^{\rm th}$ nearest neighbour, for the GZ2-BERLIND and GZ2-GROUP samples. Σ is a more direct probe of the local density of a galaxy's environment, and although it does not allow for the identification of groups and their properties, it is still a useful probe of the local density inside a group (see Muldrew et al. 2012, for a comparison of various environment parametrisations).

Here we use the estimates of Bamford et al. (2009) who averaged $\log \Sigma_N$ for $N = 4$ and $N = 5$ by the method outlined in Baldry et al. (2006), for the entirety of the GZ2 sample. We find that 90% of the GZ2-BERLIND sample have $\log \Sigma > -0.8$ (the threshold quoted by Baldry et al. 2006 to define non-field galaxies), suggesting a purity of $\sim$ 90% for the GZ2-BERLIND sample.

2.3 Field sample

We constructed a sample of field galaxies for use as a control sample to the GZ2-GROUP sample. For all galaxies in the GZ2-GALEX sample, we calculated the smallest projected group-centric radii, R/R_{200}, from each of the central galaxies in the Berlind et al. (2006) catalogue (regardless of whether the central was included in the GZ2-BERLIND sample). We also utilise the measurement of the projected neighbour density, Σ, from Baldry et al. (2006). We select candidate field galaxies as those with (i) $R/R_{200} > 25$ and (ii) $\log \Sigma < -0.8$ (the threshold on the local environment density which selects field galaxies as defined by Baldry et al. 2006). We chose to use both of these environmental density measures to ensure a pure sample of candidate field galaxies.

Firstly, each of the central galaxies of the GZ2-GROUP sample were matched to at least one candidate field galaxy in both redshift ($\pm$10%) and stellar mass ($\pm$10%), to give 2,309 field galaxies with $z < 0.084$. As with the GZ2-GROUP sample in Section 2.2 we focus on galaxies which are either quenching or quenched and are more than 1σ below the SFS and so the same constraints must be placed on this field control sample. This encompasses 1,596 field galaxies with $z < 0.084$ which will be referred to as the GZ2-CENT-FIELD-Q sample. It will be used as a control sample when investigating the inferred quenching parameters of the central galaxies of the GZ2-GROUP sample. The redshift distribution of the GZ2-CENT-FIELD-Q sample is shown in comparison to the distribution of central galaxies in the GZ2-GROUP sample in the left panel of Figure 3.

Secondly, each of the satellite galaxies of the GZ2-

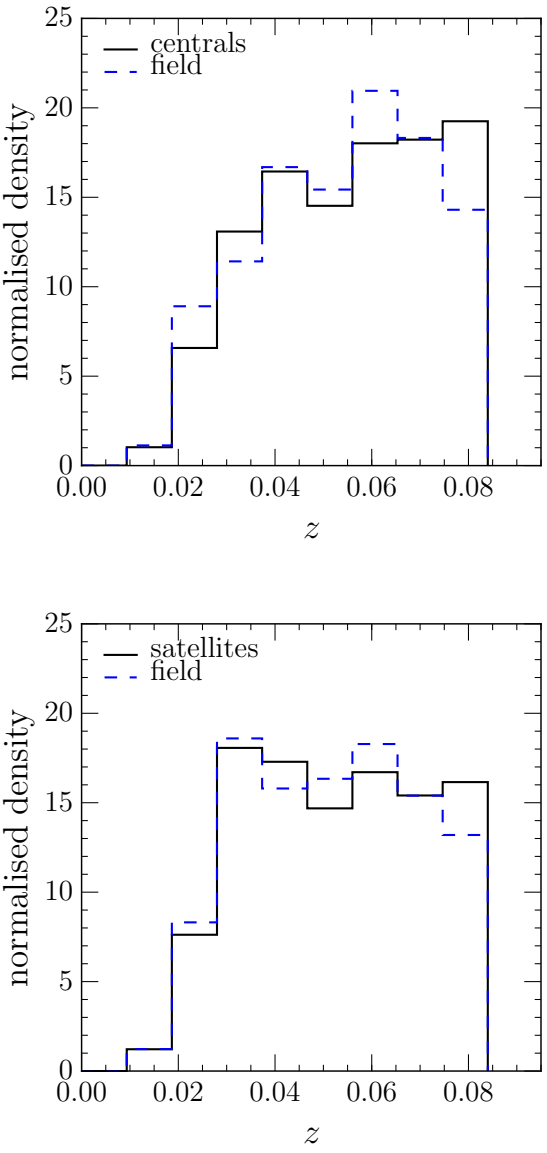

Figure 3. Redshift distributions of central galaxies in the GZ2-GROUP sample (left; black solid line) and satellite galaxies in the GZ2-BERLIND sample (right; black solid line) in comparison the redshift matched GZ2-CENT-FIELD-Q (left; blue dashed line) and GZ2-SAT-FIELD samples (right; blue dashed line).

BERLIND sample were matched to at least one candidate field galaxy in both redshift (±10%) and stellar mass (±10%), to give 5,004 field galaxies with $z < 0.084$ which will be referred to as the GZ2-SAT-FIELD sample. Note that this sample is not restricted to being 1σ below the SFS as it will be used as a control when investigating the morphological trends of satellite galaxies in the GZ2-BERLIND sample (i.e. those not restricted to being below the SFS) with environment.

237 galaxies are present in both the GZ2-CENT-FIELD-Q and GZ2-SAT-FIELD samples. The redshift distribution of the GZ2-SAT-FIELD sample is shown in comparison to the distribution of satellite galaxies in the GZ2-BERLIND sample in the right panel of Figure 3.

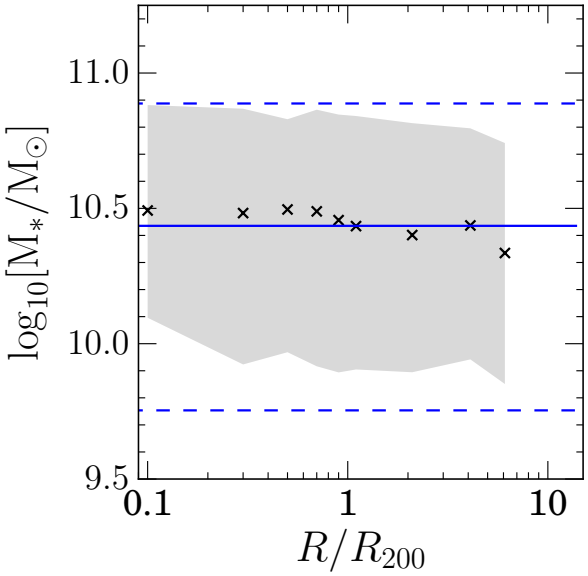

Figure 4. The median stellar mass as a function of radius from the group centre for the GZ2-BERLIND sample. The shaded regions show the range encompassing 68% of the values in each bin of R/R_{200}. The average stellar mass of the GZ2-SAT-FIELD sample is also shown (blue solid line) with the blue dashed lines bounding the range where 68% of the sample are found. The bin edges used are $R/R_{200} = [0.01, 0.2, 0.4, 0.6, 0.8, 1.0, 2.0, 4.0, 6.0, 10.0]$ and each point is plotted at the lower edge of the bin, except for the inner point which is plotted at 0.1 R/R_{200}.

We once again obtain SFRs and stellar velocity dispersions of galaxies for all of the field samples described above from the MPA-JHU catalogue (Kauffmann et al. 2003; Brinchmann et al. 2004).

3 EFFECT OF THE GROUP ENVIRONMENT ON DETAILED MORPHOLOGICAL STRUCTURE

We utilise the GZ2 vote fractions to quantify the morphology of galaxies in the GZ2-BERLIND sample, in order to investigate the morphological trends with group radius. We utilise $p_{\rm disc}$ and $p_{\rm smooth}$ to characterise the likelihood of galaxies being either discs or early-types. We also use vote fractions from further down the GZ2 decision tree including $p_{\rm bar}$, $p_{\rm bulge}$ and $p_{\rm merger}$ to calculate the bar, bulge and merger fractions in the GZ2-BERLIND sample respectively.

Fractions are calculated considering the number of barred (with $p_{\rm bar} > 0.5$; see Masters et al. 2011; Cheung et al. 2013) and bulged (with $p_{\rm obvious\ or\ dominant} > 0.5$ and $p_{\rm none\ or\ noticeable} > 0.5$) galaxies over the number of disc galaxies ($p_{\rm disc} > 0.43$, $p_{\rm edge\_on,no} > 0.715$, $N_{\rm edge\_on,no} > 20$; see Table 3 of Willett et al. 2013 for appropriate thresholds on the GZ2 vote fractions to select a sample of galaxies with a particular morphology) in the GZ2-BERLIND satellite sample. The merger fraction considers the number of merging galaxies (with $p_{\rm merger} > 0.4$; see Darg et al. 2010) over the number of galaxies in the GZ2-BERLIND satellite sample.

Since morphological features have been shown to be dependent on the stellar mass of a galaxy (e.g. the increase

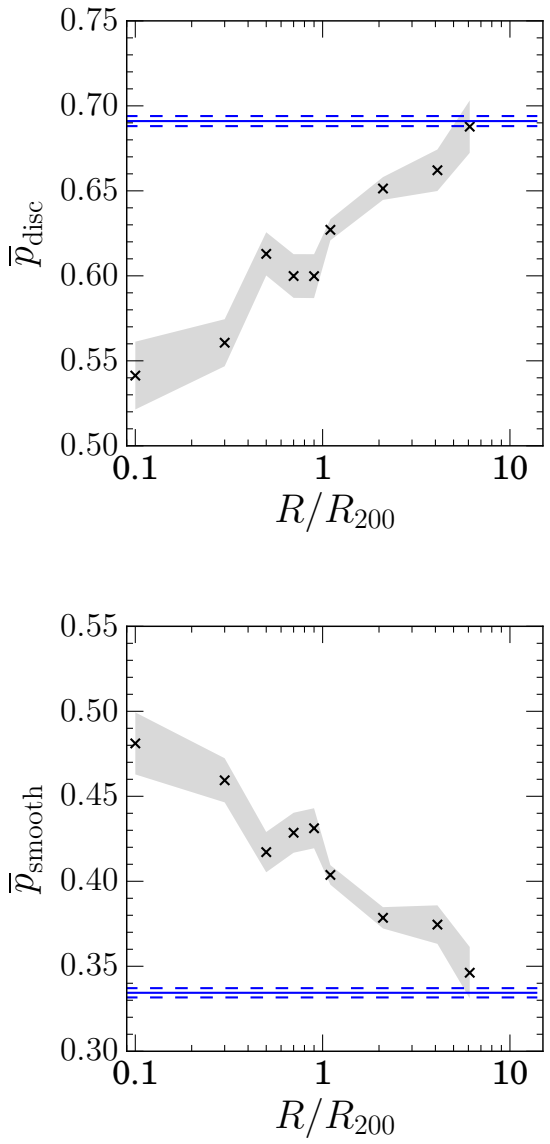

Figure 5. Mean GZ2 vote fraction for disc (top) and smooth (bottom) galaxies in the GZ2-BERLIND sample binned by projected group-centric radius, normalised by R_{200}, a proxy for the virial radius of a group. The shaded region shows $\pm1\sigma$, the standard error on the mean vote fraction. The mean vote fraction of the GZ2-SAT-FIELD sample are also shown (blue solid lines) with $\pm1\sigma$ (blue dashed lines).The bin edges used are $R/R_{200} = [0.01, 0.2, 0.4, 0.6, 0.8, 1.0, 2.0, 4.0, 6.0, 10.0]$ and each point is plotted at the lower edge of the bin, except for the inner point which is plotted at 0.1 R/R_{200}.

in the bar fraction with stellar mass; see Nair & Abraham 2010; Skibba et al. 2012), before investigating trends in the morphology with group radius in the GZ2-BERLIND sample, the mass dependence on the group radius must be considered. This is shown in Figure 4. The median stellar mass is roughly flat with increasing group radius and is consistent with the median field value. We can therefore assume that any morphological trends we observe with decreasing group radius are mass independent.

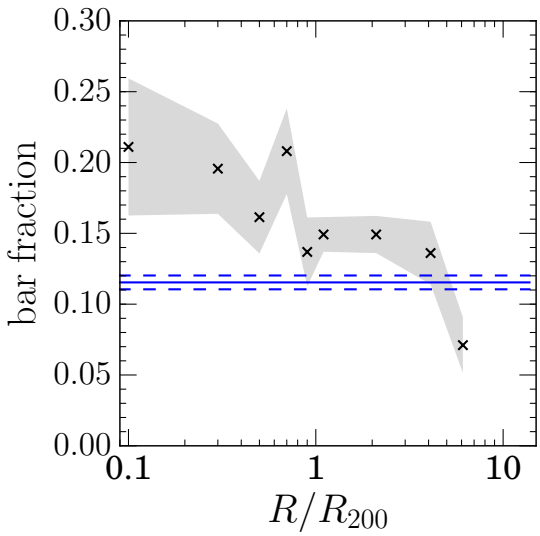

Figure 6. Bar fraction (number of barred disc galaxies over number of disc galaxies) in the GZ2-BERLIND sample binned in projected group-centric radius, normalised by R_{200}, a proxy for the virial radius of a group. The shaded region shows $\pm1\sigma$, the propagated counting error, on the bar fraction. The bar fraction of the GZ2-SAT-FIELD sample is also shown (blue solid line) with $\pm1\sigma$ (blue dashed line).The bin edges used are $R/R_{200} = [0.01, 0.2, 0.4, 0.6, 0.8, 1.0, 2.0, 4.0, 6.0, 10.0]$ and each point is plotted at the lower edge of the bin, except for the inner point which is plotted at 0.1 R/R_{200}.

3.1 Results

We perform an initial sanity check on the GZ2-BERLIND sample by recreating the morphology-density relation of Dressler (1980) in Figure 5, which shows the mean disc and smooth vote fractions as a function of group radius. The mean disc vote fraction decreases from the mean field value (blue line) within 1 R_{200}. Simultaneously, the mean smooth vote fraction increases, which is in agreement with previous studies on the morphology-density relation (Dressler 1980; Smail et al. 1997; Poggianti et al. 1999; Postman et al. 2005; Bamford et al. 2009). The extensive morphological classifications provided by GZ2 also allow for the investigation of how more detailed morphological structure is affected by the group environment.

Figure 6 shows how the bar fraction (number of barred disc galaxies over the number of disc galaxies; see Section 3) increases significantly over the field fraction (blue solid line) with decreasing group-centric radius, in agreement with the findings of Barazza et al. (2009).

In Figure 7 we show how the merger fraction does not significantly deviate from the field fraction (blue solid line) except for galaxies found at < 1 R_{200}. As discussed in Section 1.2.1, mergers are thought to drive bulge growth and so similarly, Figure 8 shows how the fraction of galaxies with obvious/dominant bulges increases over the field value at < 1 R_{200}, in the inner regions of the group (in agreement with Diaferio et al. 2001) and the fraction of those with none/just noticeable bulges decreases below the field value at < 1 R_{200}.

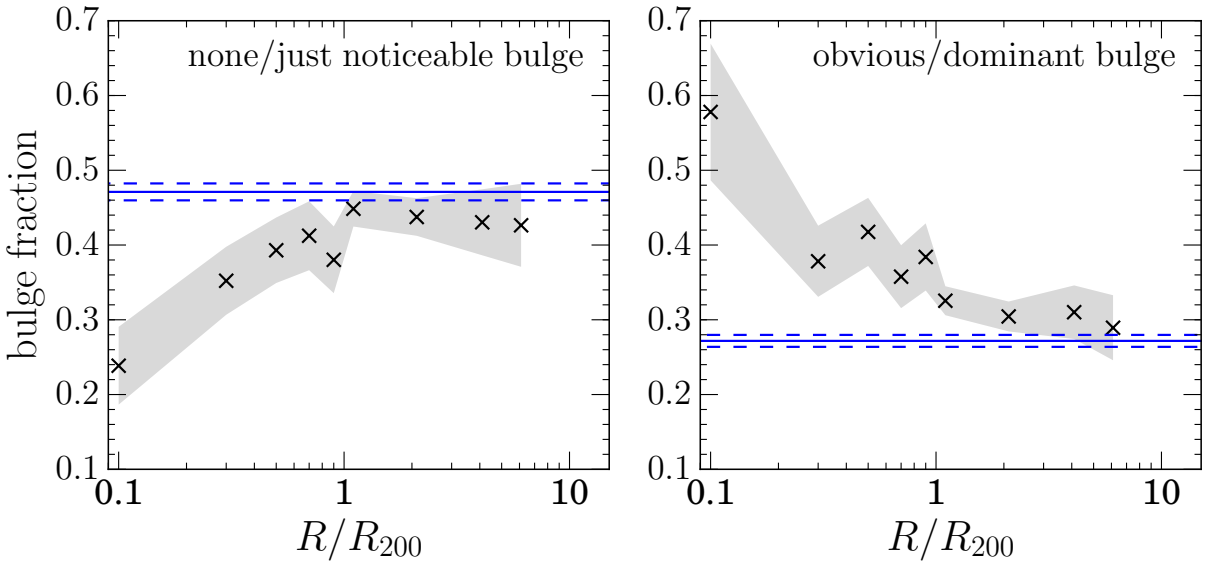

Figure 8. Fraction of galaxies with none/just noticeable bulge classifications (left) and with obvious/dominant bulge classifications (right) in the GZ2-BERLIND sample binned in projected group-centric radius, normalised by R_{200}, a proxy for the virial radius of a group. The shaded regions shows $\pm1\sigma$, the propagated counting error, on the bulge fractions. The bulge fractions of the GZ2-SAT-FIELD sample are also shown (blue solid lines) with $\pm1\sigma$ (blue dashed lines).The bin edges used are $R/R_{200} = [0.01, 0.2, 0.4, 0.6, 0.8, 1.0, 2.0, 4.0, 6.0, 10.0]$ and each point is plotted at the lower edge of the bin, except for the inner point which is plotted at 0.1 R/R_{200}.

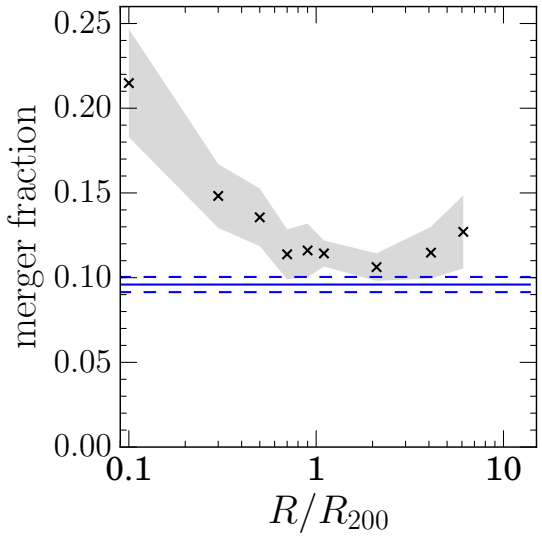

Figure 7. Merger fraction in the GZ2-BERLIND sample binned in projected group-centric radius, normalised by R_{200}, a proxy for the virial radius of a group. The shaded region shows $\pm1\sigma$, the propagated counting error, on the merger fraction. The merger fraction of the GZ2-SAT-FIELD sample is also shown (blue solid line) with $\pm1\sigma$ (blue dashed line).The bin edges used are $R/R_{200} = [0.01, 0.2, 0.4, 0.6, 0.8, 1.0, 2.0, 4.0, 6.0, 10.0]$ and each point is plotted at the lower edge of the bin, except for the inner point which is plotted at 0.1 R/R_{200}.

4 QUENCHING HISTORIES IN THE GROUP ENVIRONMENT

STARPY[2] is a PYTHON code which allows the user to derive the quenching star formation history (SFH) of a single galaxy through a Bayesian Markov Chain Monte Carlo method (Foreman-Mackey et al. 2013)[3] with the input of the observed $u-r$ and $NUV-u$ colours, a redshift, and the use of the stellar population models of Bruzual & Charlot (2003). These models are implemented using solar metallicity (varying this does not substantially affect these results; Smethurst et al. 2015) and a Chabrier IMF (Chabrier 2003) but do not model for intrinsic dust. The SFH is modelled as an exponentially declining SFR described by two parameters $[t_q, \tau]$, where t_q is the time at the onset of quenching [Gyr] and τ is the exponential rate at which quenching occurs [Gyr]. Under the simplifying assumption that all galaxies formed at $t = 0$ Gyr with an initial burst of star formation, the SFH can be described as:

$$SFR = \begin{cases} i_{sfr}(t_q) & \text{if } t < t_q \\ i_{sfr}(t_q) \times exp\left(\frac{-(t-t_q)}{\tau}\right) & \text{if } t > t_q \end{cases} \quad (4)$$

where i_{sfr} is the constant star formation rate (SFR) defined so that at the time of quenching, t_q, the modelled galaxy resides on the 'star forming sequence' (SFS). We use the definition of the SFS from Peng et al. (2010) for a galaxy with mass, $m = 10^{10.27} M_\odot$ (the mean mass of the GZ2-GALEX sample) at the redshift of the observed galaxy. A smaller τ value corresponds to a rapid quench, whereas a larger τ value corresponds to a slower quench.

[2] Publicly available: `http://github.com/zooniverse/starpy/`
[3] `http://dan.iel.fm/emcee/`

We note that a galaxy undergoing a slow quench is not necessarily quiescent by the time of observation. Similarly, despite a rapid quenching rate, star formation in a galaxy may still be ongoing at very low rates, rather than being fully quenched. This SFH model has previously been shown to appropriately characterise populations of quenching or quiescent galaxies (Weiner et al. 2006; Martin et al. 2007; Noeske et al. 2007; Schawinski et al. 2014). We note also that star forming galaxies in this regime are fit by a constant SFR with a $t_q \simeq \mathrm{Age}(z)$, (i.e. the age of the Universe at the galaxy's observed redshift) with a very low probability.

The probabilistic fitting method used to determine the star formation history for an observed galaxy is described in full detail in Section 3.2 of Smethurst et al. (2015), wherein the STARPY code was used to characterise the SFHs of each galaxy in the GZ2-GALEX sample. We assume a flat prior on all the model parameters and the difference between the observed and predicted $u-r$ and $NUV-u$ colours are modelled as independent realisations of a double Gaussian likelihood function (Equation 2 in Smethurst et al. 2015). We also make the simplifying assumption that the age of each galaxy, t_{age} corresponds to the age of the Universe at its observed redshift, t_{obs}. An example posterior probability distribution output by STARPY is shown for a single galaxy in Figure 5 in Smethurst et al. (2015), wherein the degeneracies of the SFH model can be clearly seen. These degeneracies are present for all galaxies run through STARPY therefore if differences in the distributions arise when comparing two galaxies (or two populations), this is due to intrinsic differences in their SFHs and not due to the degeneracies of the model.

We note that galaxy colours were not corrected for intrinsic dust attenuation. However, Smethurst et al. (2016, see Section 2.2) showed that internal galactic extinction does not systematically bias the results from STARPY.

The SFHs of all galaxies in both the GZ2-GROUP and GZ2-CENT-FIELD-Q samples were analysed using STARPY, providing the posterior probability distribution across the two-parameter space for each individual galaxy. In Smethurst et al. (2015) and Smethurst et al. (2016) the individual SFHs of the entire GZ2-GALEX sample and those hosting Type 2 AGN, respectively, were combined and weighted to give an overall distribution of the quenching parameters within a population of galaxies. However, in this study we take the median value of an individual posterior probability distribution (i.e. the 50th percentile position of the MCMC chain, with the $\pm1\sigma$ derived from the 16th and 84th percentile positions, see Section 3.2 of Smethurst et al. 2015) to give the most likely quenching time, t_q, and quenching rate, τ, for each galaxy. This was in order to investigate the trends in the quenching parameters with projected group centric radius.

This simplifies the output from STARPY for each galaxy from a probability distribution to just two values, with $\pm1\sigma$ uncertainties, which encompass the spread of the individual galaxy's SFH posterior probability distribution. We then calculate the time since quenching onset, Δt, for a given galaxy by calculating $\Delta t = t^{\mathrm{obs}} - t_q$ (where t^{obs} is the age of the Universe at a galaxy's observed redshift; see Section 4).

4.1 Results

With the output from STARPY we can now observe the trends in the time since quenching onset, Δt, and quenching rate, τ, with group radius, R/R_{200}, for satellite galaxies and central galaxies in the GZ2-GROUP sample, compared with galaxies in the GZ2-CENT-FIELD-Q sample. This is shown in Figures 9 - 11 wherein the GZ2-GROUP galaxies are binned by stellar mass (Figures 9a-b), halo mass (Figures 9c-d), mass ratio (Figures 10a-b), number of group galaxies (Figures 10c-d), relative velocity (Figures 11a-b) and stellar velocity dispersion (Figures 11c-d). All bin thresholds were chosen to give approximately the same number of satellite galaxies in each bin.

We quantify the trends with R/R_{200} seen across Figures 9 - 11 by performing a linear regression fit[4] (Kelly 2007) to the central bin in each figure panel. The slopes, m, derived using this method, along with $\pm1\sigma$ are provided in Table 1.

A general trend for increasing time since quenching onset, Δt with decreasing projected group-centric radius, R/R_{200}, can be seen in the left panels in Figures 9 - 11, supported by the fitted slopes stated in Table 1 which range from $-1.133 < m < -0.572$. Differences from the mean field Δt values arise at < 1 R_{200}, similar to the results found for the environmental dependence of the morphological structure (Figures 5−8). However, no trend with group radius is seen for the rate at which quenching occurs for satellites in the GZ2-GROUP sample (right panels Figures 9 - 11), supported by the fitted slopes stated in Table 1 which range from $-0.260 < m < -0.003$. This suggests that whatever mechanisms cause quenching in a group will do so at the same rate in both the dense inner and sparse outer regions.

We first split the GZ2-GROUP sample by stellar mass, M_*, and a clear trend for increasing Δt with increasing stellar mass for satellite, central and field galaxies can be seen (Figure 9a). However, this trend is less apparent for the rate that quenching occurs (Figure 9b). The central galaxies (shown by the square points) have quenched more recently than the inner satellites (at $\sim 0.1R/R_{200}$) of the same mass but have done so at the same quenching rate.

We then split the GZ2-GROUP sample by halo mass by using the stellar mass of the corresponding central galaxy of a group, $M_{cent,*}$, as a proxy. We find a clear trend for increasing time since quenching onset with increasing halo mass for satellite, central and field galaxies (Figure 9c) but this trend is absent for the rate of quenching (Figure 9d) suggesting that the halo mass does not affect which quenching mechanism acts upon either central or satellite galaxies.

To account for the effects of conformity, whereby satellites of higher mass tend to be found in higher mass halos (Weinmann et al. 2006; Kauffmann et al. 2013; Hearin et al. 2015; Hatfield & Jarvis 2016), we also split the satellites of the GZ2-GROUP sample by the stellar mass ratio of the satellite to its central galaxy, $\mu_* = M_*/M_{cent,*}$. The time since quenching onset, Δt, increases steeply with group radius (particularly within $\sim$ one virial radius; Figure 10a) particularly for satellite galaxies with much smaller masses than their group central ($-2.0 < \log_{10}\mu_* < -0.25$, shown by the blue curve). This is confirmed by the slope derived in the linear regression fit stated in Table 1, $m = -1.133\pm^{2.532}_{2.582}$,

[4] `http://linmix.readthedocs.io/`

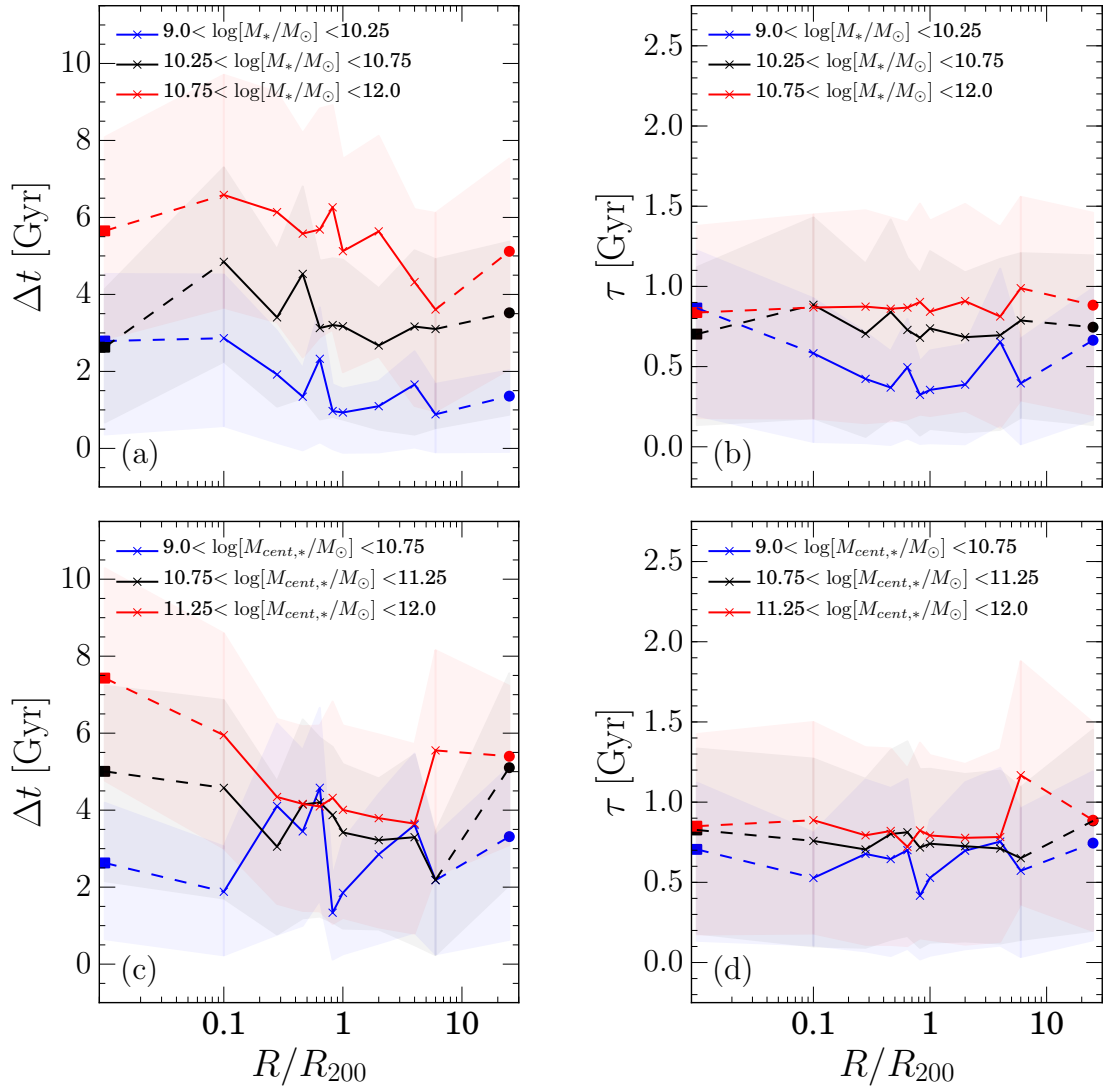

Figure 9. The median time since quenching onset ($\Delta t = t_{obs} - t_q$; left) and rate of quenching (τ; right) binned in group radius, R/R_{200}, for satellite galaxies (crosses) split into bins of stellar mass (top) and stellar mass of the corresponding central galaxy (bottom; a proxy for halo mass of a group). The corresponding values for central galaxies (squares, plotted at $\sim 0.01R/R_{200}$) and galaxies in the GZ2-CENT-FIELD-Q sample (circles, plotted at $25R/R_{200}$) are shown and connected by the dashed lines to help guide the eye. The shaded regions show the median $\pm 1\sigma$ on Δt and τ in each bin of R/R_{200}. The bin edges used are $R/R_{200} = [0.01, 0.2, 0.4, 0.6, 0.8, 1.0, 2.0, 4.0, 6.0, 10.0]$ and each point is plotted at the lower edge of the bin, except for the inner point which is plotted at 0.1 R/R_{200}.

which is the steepest slope derived for any of the parameters investigated. Once again there is no trend for the rate that quenching occurs (Figure 10b, $m = -0.097\pm^{0.519}_{0.540}$).

Another property of the group which is expected to affect the satellite quenching histories is the number of group members, N_{group}, which should be roughly correlated with a satellite's local density in a group. We find that there is no trend with time since quenching onset (Figure 10c) or rate of quenching (Figure 10d) with increasing N_{group} for satellite galaxies (however the general trend for increasing Δt with R/R_{200} is still apparent with a slope, $m = -1.052\pm^{2.560}_{2.369}$). The central galaxies (shown by the square points) however, do show a trend for increasing time since quenching as the number of group galaxies increases (Figure 10c), but the rate at which they quench is the same (Figure 10d) suggesting the mechanism by which this occurs is the same for all centrals regardless of halo mass.

The GZ2-GROUP satellite galaxies are also split into bins of their relative velocity, $|\Delta v|$ to their central galaxies, i.e. the velocity at which they move through the dense group environment. There is no trend with either time since onset of quenching (Figure 11a) or rate of quenching (Figure 11b) with increasing relative velocity for galaxies in the GZ2-GROUP sample. We remind the reader once again that these results do not change if only those galaxies inside the $(\Delta v/\sigma)\times(R/R_{200}) > 3$ caustic are used in the analysis (see Section 2.2). This suggests that whatever quenching mechanism is occurring in groups, it is not correlated with the

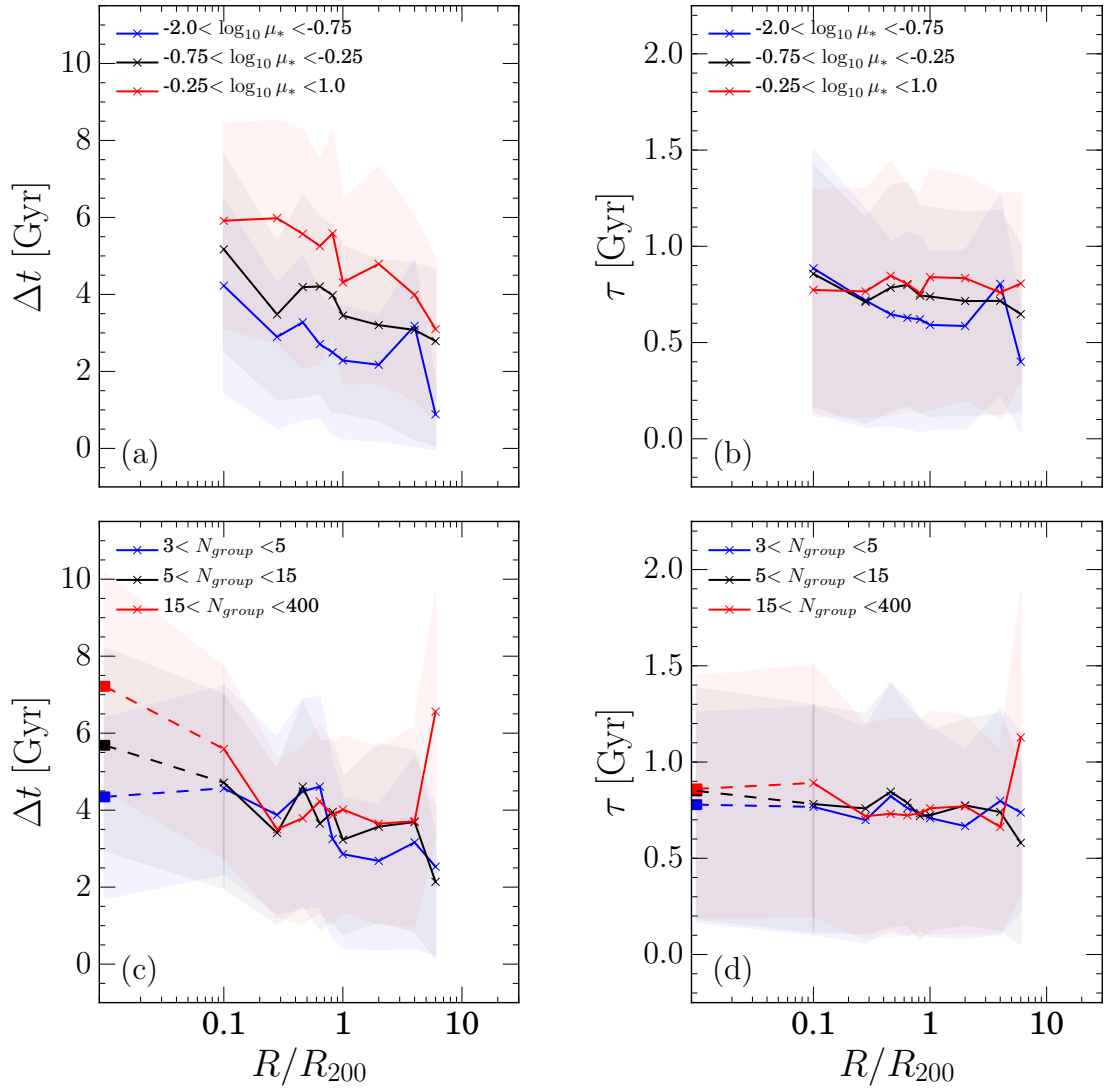

Figure 10. The median time since quenching onset ($\Delta t = t_{obs} - t_q$) and rate of quenching (τ; right) binned in group radius, R/R_{200}, for satellite galaxies (crosses) split into bins of stellar mass ratio ($\mu_* = M_*/M_{cent,*}$, top) and number of group members (N_{group}, bottom). The corresponding values for central galaxies (squares, plotted at $\sim 0.01 R/R_{200}$) and galaxies in the GZ2-CENT-FIELD-Q sample (circles, plotted at $25 R/R_{200}$) are shown, where possible, and connected by the dashed lines to help guide the eye. The shaded regions show the median $\pm 1\sigma$ on Δt and τ in each bin of R/R_{200}. The bin edges used are $R/R_{200} = [0.01, 0.2, 0.4, 0.6, 0.8, 1.0, 2.0, 4.0, 6.0, 10.0]$ and each point is plotted at the lower edge of the bin, except for the inner point which is plotted at 0.1 R/R_{200}.

Table 1. Linear regression fits are performed on the central bins of the data shown in Figures 9-11 to quantify the trends observed. The table states the median value of the posterior distribution of the inferred slope (along with $\pm 1\sigma$) when fitted to both the Δt and τ variables when the GZ2-GROUP satellite galaxies are split by the stated property. All values are quoted to 3 decimal places.

	Shown in Figure	Slope in Δt	Slope in τ
M_*	5.9a,b	$-0.699^{+2.409}_{-2.491}$	$-0.022^{+0.509}_{-0.552}$
$M_{\rm cent,*}$	5.9c,d	$-1.063^{+2.275}_{-2.350}$	$-0.090^{+0.504}_{-0.502}$
μ_*	5.10a,b	$-1.133^{+2.582}_{-2.532}$	$-0.097^{+0.540}_{-0.519}$
$N_{\rm group}$	5.10c,d	$-1.052^{+2.396}_{-2.560}$	$-0.090^{+0.492}_{-0.506}$
$\lvert\Delta v\rvert$	5.11a,b	$-0.572^{+2.534}_{-2.502}$	$-0.260^{+0.469}_{-0.465}$
σ_*	5.11c,d	$-0.647^{+2.786}_{-2.750}$	$-0.003^{+0.562}_{-0.558}$

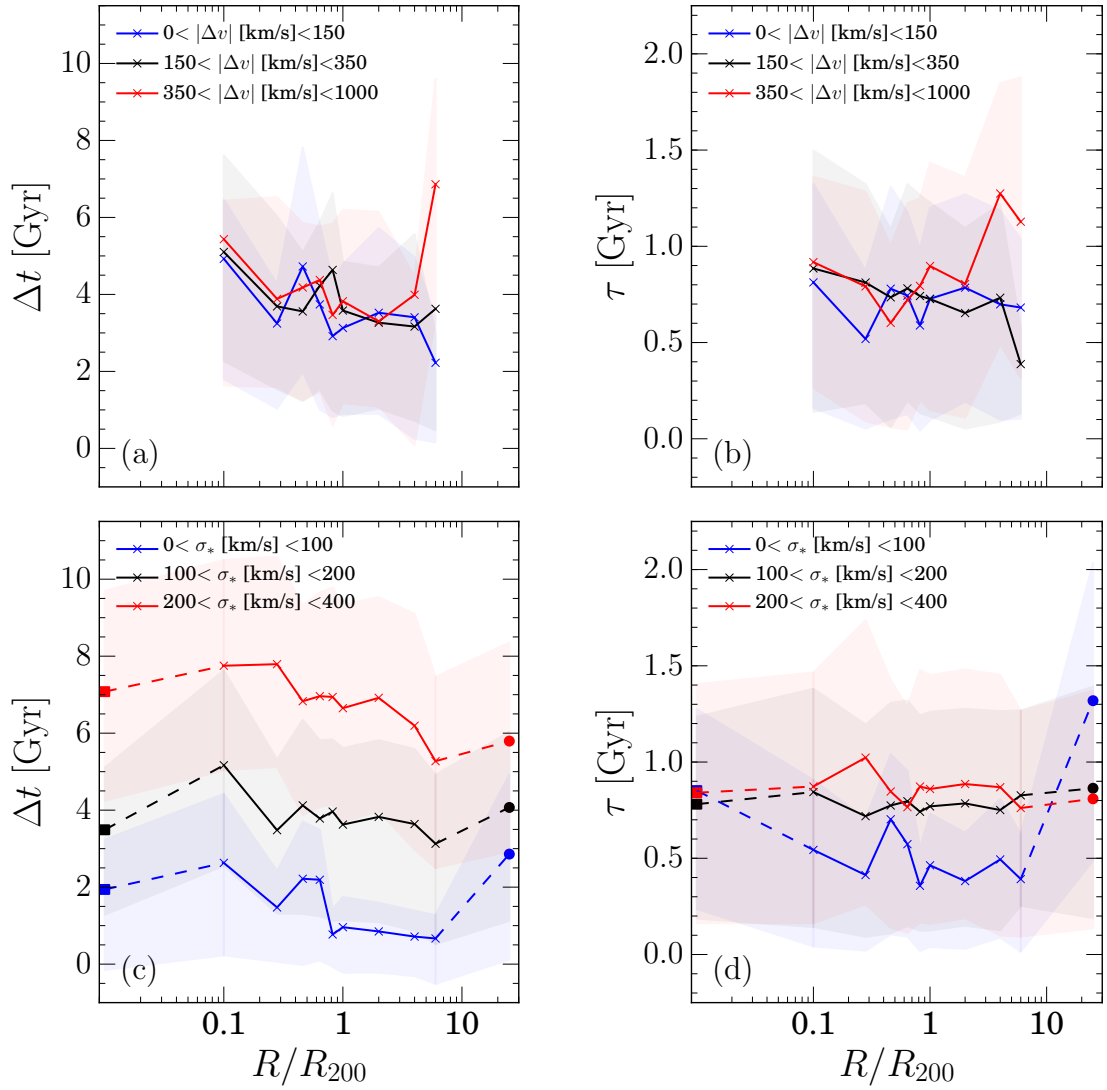

Figure 11. The median time since quenching onset ($\Delta t = t_{obs} - t_q$; left) and rate of quenching (τ; right) binned in group radius, R/R_{200}, for satellite galaxies (crosses) split by the absolute relative velocity of the satellite to its central galaxy ($|\Delta v|$, top) and stellar velocity dispersion (σ_*, bottom). The corresponding values for central galaxies (squares, plotted at $\sim 0.01 R/R_{200}$) and galaxies in the GZ2-CENT-FIELD-Q sample (circles, plotted at $25 R/R_{200}$) are shown, where possible, and connected to the satellite values by the dashed lines to help guide the eye. The shaded regions show the median $\pm 1\sigma$ on Δt and τ in each bin of R/R_{200}. The bin edges used are $R/R_{200} = [0.01, 0.2, 0.4, 0.6, 0.8, 1.0, 2.0, 4.0, 6.0, 10.0]$ and each point is plotted at the lower edge of the bin, except for the inner point which is plotted at 0.1 R/R_{200}. Note that σ_* values derived below the SDSS instrument dispersion of 70 km s^{-1} are assumed to be upper limits (see Section 2.2).

velocity at which satellites move through the dense environment.

We also investigate the trend with projected group-centric radius for the GZ2-GROUP satellites when split into bins of galaxy stellar velocity dispersion, σ_* (note that this is not the velocity dispersion of the group), which is often used as a proxy for the galaxy potential. The stellar velocity dispersion shows the largest trend in Δt (Figure 11c) for satellite galaxies in comparison to the other properties investigated (shown in Figures 9-11), with galaxies with low stellar velocity dispersions having quenched ~ 6 Gyr more recently than those with high stellar velocity dispersion. Although this trend is less apparent for the rate that quenching occurs when the satellite galaxies are split by σ_* (Figure 11d), it is the largest trend seen in the rate of quenching for any of the properties investigated (shown in the right panels of Figures 9-11). Also, field galaxies (shown by the circles at $\sim 25 R/R_{200}$ in 11d) with low velocity dispersions are seen to quench at much slower rates than their satellite counterparts ($\tau \sim 1.3$ Gyr versus $\tau \sim 0.5$ Gyr). This suggests that the rapid quenching observed for the low stellar velocity dispersion satellites is directly caused by the environment.

5 DISCUSSION

We shall now consider the results presented in Sections 3 & 4 in the context of the possible quenching mechanisms which could be responsible. We focus on those mechanisms first introduced in Sections 1.1 & 1.2.

5.1 The role of mergers as quenching mechanisms in the group environment

The merger classification in GZ2 has been shown to preferentially identify major mergers (Darg et al. 2010); while bulge formation in disc galaxies is often associated with evolutionary histories driven by minor mergers (Croton et al. 2006; Tonini et al. 2016). Although we see evidence for an enhanced merger fraction in the inner regions of the group environment (Figure 7), the bulge fractions vary much more significantly from the field value than the merger fraction (Figure 8). This suggests that minor mergers may be more dominant than major mergers for satellites in the group environment, particularly at $R/R_{200} > 0.5$.

If mergers are a dominant evolutionary mechanism for satellite galaxies (as the morphological evidence in Figures 7 & 8 suggests) we would expect to see a difference in the quenching histories of satellites residing in groups with a larger number of members. However, there is no trend with time since quenching onset (Figure 10c) or rate of quenching (Figure 10d) with increasing N_{group} for the satellite galaxies. This suggests that mergers are not the dominant quenching mechanism for satellite galaxies, but that whatever mechanism is the cause of the quenching occurs at the same rate irrespective of group size.

Central galaxies however, do show a trend for increasing time since quenching with increasing N_{group} (square points in Figure 10c) occurring at a rate of $\tau \sim 0.8$Gyr. Smethurst et al. (2015) attributed these quenching rates to mergers and galaxy interactions which can transform a galaxy's morphology. Therefore, the larger the number of group members, the more likely a central galaxy has a history dominated by mergers. This is in agreement with the findings of Lin et al. (2010), Ellison et al. (2010), Lidman et al. (2013) and McIntosh et al. (2008). The latter found, by studying a sample of local groups and clusters, that half of the mergers they identified involved the central galaxy. Liu et al. (2009) also found that the fraction of merging centrals increases with the richness of a cluster (a measure of the number of galaxies within 1 h^{-1}Mpc of the central galaxy).

This idea is supported by the result that centrals of a given mass have quenched more recently than the inner satellites (at $\sim 0.1R/R_{200}$ in Figure 9a) of a given mass. This suggests that an episode of more recent star formation, such as a starburst, may have occurred in the central galaxies but not in the inner satellites. Mergers are thought to cause an energetic burst of star formation which can in turn quench the remnant galaxy (Hopkins et al. 2005; Treister et al. 2012; Pontzen et al. 2016). This result is supportive of a merger dominated history for central galaxies but not for satellite galaxies.

5.2 The role of mass quenching in the group environment

A trend is seen for increasing time since quenching with increasing stellar mass and velocity dispersion (a proxy for galaxy potential) for centrals, satellites and field galaxies in Figure 9a and Figure 11c respectively. This is suggestive of mass quenching occurring across the entire galaxy population irrespective of environmental density, supporting the work of Peng et al. (2010, 2012); Gabor et al. (2010) and Darvish et al. (2016).

5.3 The role of morphological quenching in the group environment

We find an increasing bar fraction toward the central group regions in agreement with Skibba et al. (2012) (Figure 6). This increase coincides with an increase in time since quenching onset with projected group radius across the satellite galaxies of the GZ2-GROUP sample (Figures 9-11 and quantified in Table 1). This suggests that bars may be partly responsible for the relation between quenched fraction and environmental density. This is consistent with findings that show that bars themselves may be the cause of morphological quenching through the funnelling of gas toward the central regions of galaxies (Athanassoula 1992b; Sheth et al. 2005) which is then used in star formation, exhausting the available gas (see Section 1.1.2).

We must therefore consider whether the environment itself may play a role in triggering the disk instabilities which can produce a bar. Indeed harassment and tidal interactions, believed to be common in the group environment, have been shown to both promote and inhibit bar formation dependent on the stellar mass (Noguchi 1988; Moore et al. 1996; Skibba et al. 2012). If the environment was indeed triggering a bar, then morphological quenching would be occurring in the group environment but indirectly due to environmental quenching. This suggests that the polarity between internal secular processes ('nature') and external environmental processes ('nurture') may not be as extreme as first thought, in agreement with Skibba et al. (2012).

5.4 The role of the environment in quenching

A trend for increasing time since quenching onset, Δt, with decreasing projected group-centric radius is present across the satellite population of the GZ2-GROUP sample (Figures 9-11 and quantified in Table 1). We interpret this as environmentally driven mechanisms causing quenching at the same rate throughout the infall time of a galaxy in a group. Galaxies which are now closer in fell into the group earlier and as they did so they started to quench, giving rise to a larger inferred Δt.

We explain this in the context of works which consider the effects of halo mass on group galaxies. More massive halos are seen to have a greater impact on the star formation histories of their satellites than less massive halos in Figure 9c. The halo mass is correlated with both (i) the gravitational potential of the group and (ii) the temperature of the IGM, suggesting that an environmental quenching mechanism which is correlated with one or both of these properties is responsible for this result.

Higher mass halos have hotter intra group medium (IGM) temperatures (Shimizu et al. 2003; Del Popolo et al. 2005) which can have a greater impact on a galaxy through ram pressure stripping (RPS) of cold gas. Gunn & Gott (1972) define the ram pressure as:

$$\rho_{\rm IGM} \cdot v^2 = 2\pi G \cdot \sigma_*(R) \cdot \sigma_g(R), \quad (5)$$

where $\rho_{\rm IGM}$ is the density of the IGM, $\sigma_*(R)$ the star surface density, $\sigma_g(R)$ the gas surface density of the galaxy disc and v the velocity of the galaxy through the IGM. Therefore if RPS is indeed a dominant environmental quenching mechanism we should see an increase in Δt with the velocity of a satellite relative to its central galaxy. However we find that this is not the case (see Figure 11a). This therefore rules out RPS as the dominant environmental quenching mechanism, in support of the simulations of Emerick et al. (2016); Fillingham et al. (2016) which showed that RPS could only remove $40-60\%$ of a satellite's gas. However, this conclusion may be due to the stellar mass range spanned by the GZ2-GROUP satellite galaxies which all have $M_* \geqslant 10^9 {\rm M}_\odot$, as simulations by Fillingham et al. (2016) suggest that RPS only becomes effective in lower mass satellites with $M_* \leqslant 10^{8-9} {\rm M}_\odot$, in agreement with Hester (2006).

Above this mass threshold in the simulations of Fillingham et al. (2016), a 'starvation' (or strangulation) mode (Larson et al. 1980; Balogh et al. 2000) dominates, where a galaxy's extended gaseous halo is removed causing a quench, as cold gas for use in star formation can no longer be fed from the extended halo. This idea is supported by observations by Peng et al. (2010) which show that strangulation is a dominant mechanism for galaxies with $M_* < 10^{11}\ M_\odot$ with a quenching timescale of 4 Gyr. Such a mechanism will be correlated with the galaxy potential, as galaxies with a lower potential will be most easily stripped of their halos. We find that satellites with lower velocity dispersion (a proxy for the galaxy potential) are more rapidly quenched than their higher velocity dispersion counterparts and those in the field (see Figure 11d). Such a starvation mechanism is also correlated with halo mass, for which similar trends in Δt are seen (Figure 9c). The dominant environmental quenching mechanism occurring in the group environment must therefore be correlated with the group potential. This suggests that satellite galaxies may be most affected by gravitationally driven environmental effects, such as starvation, thermal evaporation of the galaxy halo and galaxy harassment.

We can calculate an infall timescale for the satellite galaxies in the GZ2-GROUP sample if we assume that galaxies begin their infall into a group at a radius of $\sim 10{\rm R}_{200}$ and stop infalling at $\sim 0.1{\rm R}_{200}$[5]. The difference in the time since quenching onset, Δt, between these two locations in a group will provide an estimate for how long it takes a satellite to infall. This assumes (i) that the galaxy starts to quench immediately when it enters the group and (ii) that the same environmentally driven quenching process is the only quenching mechanism affecting the satellites throughout their infall. We estimate this infall time by calculating the difference in Δt at 0.1 R_{200} and at ~ 10 R_{200} found in a given bin for each curve shown across Figures 9-11. We define this property as $\delta\Delta t = \Delta t_{0.1R_{200}} - \Delta t_{10R_{200}}$.

We therefore estimate a median infall time of $\delta\Delta t \sim 2.4$ Gyr for the GZ2-GROUP satellites. Similarly, the median rate of quenching of the GZ2-GROUP satellites is $\tau \sim 0.8$ Gyr (which is within the range of quenching rates hypothesised to cause a morphological change by Smethurst et al. 2015) and so we can also estimate the median quenching timescale (i.e. the time taken to fully quench from the SFS to 5σ below the SFS) to be ~ 2.5 Gyr for the GZ2-GROUP satellites (increasing to ~ 5.3 Gyr for those galaxies with $\tau \sim 1.5$Gyr).

This infall time and quenching timescale are in agreement with the estimates of Wetzel et al. (2013) who used a high resolution cosmological N-body simulation to track satellite galaxy orbits in SDSS groups and clusters and found quenching timescales of $2-6$ Gyr. Using a similar method, Oman & Hudson (2016) derive an infall time of ~ 4 Gyr and quenching timescales between $4-6$ Gyr for galaxies in the mass range of the GZ2-GROUP sample. Similarly, Hahn et al. (2016) derive a total quenching timescale of ~ 4 Gyr for satellite galaxies on infall into the group environment. However, the simulations by Fillingham et al. (2016) and Emerick et al. (2016) have shown that RPS cannot remove enough gas mass to completely quench a galaxy within ~ 2 Gyr but can assist in reducing the starvation timescale so that galaxies can be quenched within ~ 4 Gyr. This suggests that although the effects of mechanisms correlating with the group potential are detectable in the quenching parameters of the GZ2-GROUP sample, this is only made possible by the constantly present, but less dominant effects of ram pressure stripping.

In Section 5.3 we also noted that morphological quenching may only be present in the group environment due to the influence of the environment itself. Considering both this pairing of the environment and morphological quenching, and the pairing of ram pressure stripping and strangulation discussed above, suggests that all the mechanisms discussed here will affect a galaxy which is infalling through the group environment at some point in its lifetime. A single mechanism may be more dominant in the evolution of an individual galaxy but to achieve the correlations between morphology, colour and quenched galaxy fraction with density observed across the entire population, all mechanisms need to act in concert.

5.5 The bigger picture of quenching in galaxies

Having discussed the results presented here, we now consider the results in this paper in a broader context in conjunction with previous results found using the STARPY method. Smethurst et al. (2015) infer the SFHs of the entire GZ2-GALEX sample using STARPY and investigate the morphological dependence of the derived quenching parameters for galaxy populations across the colour magnitude diagram. They find a clear difference between the quenching rates preferred by smooth and disc populations with smooth galaxies transitioning the green valley at faster rates than disc galaxies. However, intermediate quenching rates with $1 < \tau[{\rm Gyr}] < 2$, similar to the rates inferred in this study in Section 4, are dominant for all morphologies across the colour-magnitude diagram. Similarly, Smethurst et al.

[5] This assumes that galaxies will then merge with their central galaxy, however it is more likely that the satellite has a close pass with the central before it 'backsplashes' into the group. See, for example, Pimbblet (2011).

(2016) infer the SFHs of GZ2-GALEX galaxies hosting optically selected Type 2 AGN and compare them to a control sample of currently inactive galaxies. They find evidence for rapid, recent quenching across the population of AGN host galaxies, particularly for galaxies with $M_* < 10.75 M_\odot$. This suggests that AGN feedback is important in the AGN host galaxy population. However, slow quenching rates are dominant for higher mass AGN host galaxies, suggesting secular evolution is also key in the evolution of galaxies currently hosting an AGN.

A parameter which is often investigated in quenching studies is the stellar mass surface density of a galaxy, which is found to correlate with SFR (Barro et al. 2013; Whitaker et al. 2016). As a galaxy's bulge grows it is thought to be able to stabilise a disc against collapse and effectively stop it from forming stars. This is classed as a type of morphological quenching and is effective over time periods of a few Gyr (Fang et al. 2013) even if external gas is still fed to a galaxy. This slower quenching track of bulge dominated galaxies may help to explain the slow quenching rates observed by Smethurst et al. (2015) across the red and green smooth populations. They find that slow quenching with $\tau > 2$ Gyr occurs for up to 40% of the smooth green population and 24% of the smooth red population. Using STARPY, Smethurst et al. (2015) separated galaxies characterised by this slower quenching history, caused by processes which grow the bulge then consequently trigger morphological quenching, from those characterised by more rapid quenching histories, which are caused by processes which simultaneously quench the galaxy and grow the bulge. However, even in the latter case, morphological quenching may help in either speeding up the quenching process or in ensuring the galaxy stays quenched. This is supported by the finding of Abramson et al. (2016) who found that there is no threshold at which density triggered quenching occurs, but that denser systems redden faster than their less dense counterparts. This suggests that minor mergers and morphological quenching work together to fully achieve quiescence, similar to the collaboration between starvation and stripping to achieve quiescence of satellite galaxies discussed in Section 5.4.

This sort of partnership between two quenching mechanisms is also apparent in simulations which have shown that without AGN feedback a major merger cannot fully quench a galaxy (Springel et al. 2005). In combination with a major merger however, a massive galaxy can be completely quenched by the heating or removal of gas and quiescence maintained (Conselice 2003; Springel et al. 2005; Hopkins et al. 2008b; Pontzen et al. 2016). These effects are therefore easily detectable, leading to the initial theories for the links between AGN and mergers (Merritt & Ferrarese 2001; Hopkins et al. 2006b, 2008b,a; Peng 2007; Jahnke & Macciò 2011). However, Smethurst et al. (2016) showed using STARPY that galaxies hosting an AGN don't always quench at the rapid rates caused by major mergers, suggesting that a slow co-evolution of black hole and host galaxy can occur. They also showed that rapid quenching is only inferred for low mass AGN host galaxies where the AGN can have a greater impact on the galaxy SFR.

Across the entire galaxy population we therefore have lots of examples of two quenching mechanisms working together to either quench a galaxy or ensure a galaxy stays quenched, including starvation and stripping (Section 5.4), disc instabilities & environment (Section 5.3), minor mergers & morphological quenching (Section 5.5) and mergers & AGN (Smethurst et al. 2015, 2016). All of these mechanisms result in the same end state of galaxy quiescence (with the occasional influx of gas thwarting their progress) but no single mechanism dominates over another, except in the most extreme environments or masses. While the effects of mass and morphological quenching are more apparent for galaxies in less dense environments (Figures 9-11), they still affect galaxies in the densest environments. Similarly, the effects of mergers are much more apparent in galaxies in dense environments (e.g. centrals; see Section 5.1) and will often drown out the more subtle effects of slower quenching mechanisms which occurred before the merger.

Just as the morphology of galaxies is continuous in nature from disc to bulge dominated, so too are the effects of the quenching mechanisms which can cause this change. The impact of mergers on the morphology and SFR of a galaxy depends on the mass ratio, a continuous variable from "micro mergers" (Carlin et al. 2016) through to major mergers. The strength of morphological quenching mechanisms can be measured on a continuum of stellar mass and stellar mass surface density of a galaxy; similarly the impact of environmentally driven quenching mechanisms increases with increasing halo mass. All of these processes, depending on a galaxy's environment, are likely to affect a galaxy at some point in its lifetime, acting in concert to reduce the SFR, which in turn produces the wide distribution of quenching timescales seen across the GZ2-GROUP sample. In previous works, efforts have been made to identify the dominant quenching mechanism in a galaxy sample (e.g. Muzzin et al. 2012; Schawinski et al. 2014; Foltz et al. 2015; Woo et al. 2015; Balogh et al. 2016; Darvish et al. 2016; Huertas-Company et al. 2016), yet it is clear from this study that multiple quenching mechanisms will affect galaxies across their lifetime, working in collaboration to ensure galaxies stay quenched. Future studies should therefore focus on disentangling the effects of these various different quenching mechanisms, rather than focussing on a single process.

6 CONCLUSIONS

Using the Berlind et al. (2006) group catalogue, we have constructed a sample of group galaxies in the SDSS which were cross matched with Galaxy Zoo 2 and GALEX in order to determine their most likely SFHs using a Bayesian MCMC code, STARPY. We have shown that although mass quenching, morphological quenching and mergers are all important mechanisms at work in quenching the galaxies in the group environment, environmentally driven quenching mechanisms do play a role in quenching galaxies as they infall into the group. We have discussed the possibility that no single mechanism will dominate across the group population, with all mechanisms acting collaboratively. Our findings are summarised as follows:

(i) The bar, obvious bulge and merger fractions are all seen to increase above the field value in the inner regions of the groups of the GZ2-GROUP sample in Figures 6, 8 & 7 respectively.

(ii) Mergers are the dominant quenching mechanism for central galaxies but not for satellite galaxies. Satellites may undergo a minor merger in the group environment but their effects are only discernible by their indirect effect on the bulge fraction (see Figure 8).

(iii) Mass dependent quenching is occurring across the entire GZ2-GROUP sample for both centrals and satellites irrespective of the environmental density (see Figure 9a).

(iv) Morphological quenching is occurring for GZ2-GROUP satellite galaxies as evidenced by the heightened bar fraction in the inner group regions (see Figure 6). However, this may be indirectly due to environmental quenching since galaxy interactions and harassment are believed to be able to trigger bars. This suggests the polarity between 'nature' vs. 'nurture' may not be as extreme as previously thought, in agreement with Skibba et al. (2012).

(v) The environment does cause quenching across the GZ2-GROUP sample, as evidenced by the increase in the time since quenching with decreasing group radius (Figures 9-11 and Table 1). Our results suggest that this is caused by a quenching mechanism correlated with the group potential, such as harassment, interactions and starvation, rather than the velocity of a satellite through the group, such as ram pressure stripping (Figures 9a & 11c). This quenching occurs within an median quenching timescale of ~ 2.5 Gyr from star forming to complete quiescence, after an average infall time of ~ 2.4 Gyr.

It is apparent from the results presented here that many quenching mechanisms are all occurring simultaneously in the group environment; therefore a superposition of all of the effects of these mechanisms is seen in the quenching histories of the GZ2-GROUP sample, which in turn gives rise to the observed morphology-density relation.

ACKNOWLEDGEMENTS

The authors would like to thank R. Davies and K. Pimbblet for discussion and suggestions which greatly improved the clarity of this paper.

RS acknowledges funding from the Science and Technology Facilities Council Grant Code ST/K502236/1.

The development of Galaxy Zoo was supported in part by the Alfred P. Sloan Foundation. Galaxy Zoo was supported by The Leverhulme Trust.

Based on observations made with the NASA Galaxy Evolution Explorer. GALEX is operated for NASA by the California Institute of Technology under NASA contract NAS5-98034

Funding for the SDSS and SDSS-II has been provided by the Alfred P. Sloan Foundation, the Participating Institutions, the National Science Foundation, the U.S. Department of Energy, the National Aeronautics and Space Administration, the Japanese Monbukagakusho, the Max Planck Society, and the Higher Education Funding Council for England. The SDSS Web Site is `http://www.sdss.org/`. The SDSS is managed by the Astrophysical Research Consortium for the Participating Institutions. The Participating Institutions are the American Museum of Natural History, Astrophysical Institute Potsdam, University of Basel, University of Cambridge, Case Western Reserve University, University of Chicago, Drexel University, Fermilab, the Institute for Advanced Study, the Japan Participation Group, Johns Hopkins University, the Joint Institute for Nuclear Astrophysics, the Kavli Institute for Particle Astrophysics and Cosmology, the Korean Scientist Group, the Chinese Academy of Sciences (LAMOST), Los Alamos National Laboratory, the Max-Planck-Institute for Astronomy (MPIA), the Max-Planck-Institute for Astrophysics (MPA), New Mexico State University, Ohio State University, University of Pittsburgh, University of Portsmouth, Princeton University, the United States Naval Observatory, and the University of Washington.

This publication made extensive use of the Tool for Operations on Catalogues And Tables (TOPCAT; Taylor 2005) which can be found at `http://www.star.bris.ac.uk/~mbt/topcat/` and the open source Python module *astroPy*[6]; Astropy Collaboration et al. 2013). This research has also made use of NASA's ADS service and Cornell's ArXiv.

REFERENCES

Abadi M. G., Moore B., Bower R. G., 1999, MNRAS, 308, 947
Abazajian K. N. et al., 2009, ApJS, 182, 543
Abell G. O., 1958, ApJS, 3, 211
Abramson L. E., Gladders M. D., Dressler A., Oemler A., Poggianti B., Vulcani B., 2016, ArXiv e-prints, 1604.00016
Astropy Collaboration et al., 2013, A&A, 558, A33
Athanassoula E., 1992a, MNRAS, 259, 328
Athanassoula E., 1992b, MNRAS, 259, 345
Athanassoula E., Rodionov S. A., Peschken N., Lambert J. C., 2016, ApJ, 821, 90
Baldry I. K., Balogh M. L., Bower R. G., Glazebrook K., Nichol R. C., Bamford S. P., Budavari T., 2006, MNRAS, 373, 469
Balogh M. L. et al., 2016, MNRAS, 456, 4364
Balogh M. L., Navarro J. F., Morris S. L., 2000, ApJ, 540, 113
Bamford S. P. et al., 2009, MNRAS, 393, 1324
Barazza F. D. et al., 2009, A&A, 497, 713
Barnes J. E., Hernquist L., 1996, ApJ, 471, 115
Barro G. et al., 2013, ApJ, 765, 104
Baugh C. M., Cole S., Frenk C. S., Lacey C. G., 1998, ApJ, 498, 504
Baugh C. M., Lacey C. G., Frenk C. S., Granato G. L., Silva L., Bressan A., Benson A. J., Cole S., 2005, MNRAS, 356, 1191
Bell E. F., Phleps S., Somerville R. S., Wolf C., Borch A., Meisenheimer K., 2006, ApJ, 652, 270
Berlind A. A. et al., 2006, ApJS, 167, 1
Bialas D., Lisker T., Olczak C., Spurzem R., Kotulla R., 2015, A&A, 576, A103
Birnboim Y., Dekel A., 2003, MNRAS, 345, 349
Blanton M. R., Eisenstein D., Hogg D. W., Schlegel D. J., Brinkmann J., 2005, ApJ, 629, 143
Blanton M. R., Roweis S., 2007, AJ, 133, 734
Bluck A. F. L., Mendel J. T., Ellison S. L., Moreno J., Simard L., Patton D. R., Starkenburg E., 2014, MNRAS, 441, 599

[6] `http://www.astropy.org/`

Bower R. G., Balogh M. L., 2004, Clusters of Galaxies: Probes of Cosmological Structure and Galaxy Evolution, 325
Bower R. G., Benson A. J., Malbon R., Helly J. C., Frenk C. S., Baugh C. M., Cole S., Lacey C. G., 2006, MNRAS, 370, 645
Brinchmann J., Charlot S., White S. D. M., Tremonti C., Kauffmann G., Heckman T., Brinkmann J., 2004, MNRAS, 351, 1151
Bruzual G., Charlot S., 2003, MNRAS, 344, 1000
Butcher H., Oemler, Jr. A., 1978, ApJ, 226, 559
Cardelli J. A., Clayton G. C., Mathis J. S., 1989, ApJ, 345, 245
Carlberg R. G., 2004, Clusters of Galaxies: Probes of Cosmological Structure and Galaxy Evolution, 343
Carlin J. L. et al., 2016, ApJ, 828, L5
Chabrier G., 2003, PASP, 115, 763
Cheung E. et al., 2013, ApJ, 779, 162
Conselice C. J., 2003, ApJS, 147, 1
Cowie L. L., Barger A. J., 2008, ApJ, 686, 72
Cowie L. L., Songaila A., 1977, Nature, 266, 501
Cox T. J., Younger J., Hernquist L., Hopkins P. F., 2008, in IAU Symposium, Vol. 245, Formation and Evolution of Galaxy Bulges, Bureau M., Athanassoula E., Barbuy B., eds., pp. 63–66
Croton D. J. et al., 2006, MNRAS, 365, 11
Cucciati O. et al., 2010, A&A, 520, A42
Darg D. W. et al., 2010, MNRAS, 401, 1043
Darvish B., Mobasher B., Sobral D., Rettura A., Scoville N., Faisst A., Capak P., 2016, ApJ, 825, 113
Dekel A., Birnboim Y., 2006, MNRAS, 368, 2
Del Popolo A., Hiotelis N., Peñarrubia J., 2005, ApJ, 628, 76
Di Matteo T., Springel V., Hernquist L., 2005, Nature, 433, 604
Diaferio A., Kauffmann G., Balogh M. L., White S. D. M., Schade D., Ellingson E., 2001, MNRAS, 323, 999
Dressler A., 1980, ApJ, 236, 351
Dressler A., 2004, in IAU Colloq. 195: Outskirts of Galaxy Clusters: Intense Life in the Suburbs, Diaferio A., ed., pp. 341–346
Eke V. R. et al., 2004, MNRAS, 348, 866
Ellison S. L., Patton D. R., Simard L., McConnachie A. W., Baldry I. K., Mendel J. T., 2010, MNRAS, 407, 1514
Emerick A., Mac Low M.-M., Grcevich J., Gatto A., 2016, ApJ, 826, 148
Fabian A. C., 2012, ARA&A, 50, 455
Fang J. J., Faber S. M., Koo D. C., Dekel A., 2013, ApJ, 776, 63
Fillingham S. P., Cooper M. C., Pace A. B., Boylan-Kolchin M., Bullock J. S., Garrison-Kimmel S., Wheeler C., 2016, MNRAS
Finn R. A. et al., 2005, ApJ, 630, 206
Foltz R. et al., 2015, ApJ, 812, 138
Foreman-Mackey D., Hogg D. W., Lang D., Goodman J., 2013, PASP, 125, 306
Gabor J. M., Davé R., 2015, MNRAS, 447, 374
Gabor J. M., Davé R., Finlator K., Oppenheimer B. D., 2010, MNRAS, 407, 749
Gómez P. L. et al., 2003, ApJ, 584, 210
Gunn J. E., Gott, III J. R., 1972, ApJ, 176, 1
Hahn C., Tinker J. L., Wetzel A. R., 2016, ArXiv e-prints, 1609.04398
Häring N., Rix H.-W., 2004, ApJ, 604, L89
Hatfield P. W., Jarvis M. J., 2016, ArXiv e-prints, 1606.08989
Hayward C. C., Torrey P., Springel V., Hernquist L., Vogelsberger M., 2014, MNRAS, 442, 1992
Hearin A. P., Watson D. F., van den Bosch F. C., 2015, MNRAS, 452, 1958
Hester J. A., 2006, ApJ, 647, 910
Hickox R. C. et al., 2009, ApJ, 696, 891
Hirschmann M., De Lucia G., Wilman D., Weinmann S., Iovino A., Cucciati O., Zibetti S., Villalobos Á., 2014, MNRAS, 444, 2938
Hopkins P. F., Cox T. J., Kereš D., Hernquist L., 2008a, ApJS, 175, 390
Hopkins P. F., Cox T. J., Younger J. D., Hernquist L., 2009, ApJ, 691, 1168
Hopkins P. F., Hernquist L., 2009, ApJ, 694, 599
Hopkins P. F., Hernquist L., Cox T. J., Di Matteo T., Robertson B., Springel V., 2006a, ApJS, 163, 1
Hopkins P. F., Hernquist L., Cox T. J., Kereš D., 2008b, ApJS, 175, 356
Hopkins P. F. et al., 2005, in Bulletin of the American Astronomical Society, Vol. 37, American Astronomical Society Meeting Abstracts, p. 1354
Hopkins P. F., Kereš D., Murray N., Quataert E., Hernquist L., 2012, MNRAS, 427, 968
Hopkins P. F., Somerville R. S., Hernquist L., Cox T. J., Robertson B., Li Y., 2006b, ApJ, 652, 864
Huertas-Company M. et al., 2016, MNRAS, 462, 4495
Jahnke K., Macciò A. V., 2011, ApJ, 734, 92
Jarosik N. et al., 2011, ApJS, 192, 14
Jones L. R., Ponman T. J., Forbes D. A., 2000, MNRAS, 312, 139
Jones L. R., Ponman T. J., Horton A., Babul A., Ebeling H., Burke D. J., 2003, MNRAS, 343, 627
Kauffmann G., 1996, MNRAS, 281, 487
Kauffmann G., Colberg J. M., Diaferio A., White S. D. M., 1999a, MNRAS, 303, 188
Kauffmann G., Colberg J. M., Diaferio A., White S. D. M., 1999b, MNRAS, 307, 529
Kauffmann G. et al., 2003, MNRAS, 341, 33
Kauffmann G., Li C., Zhang W., Weinmann S., 2013, MNRAS, 430, 1447
Kelly B. C., 2007, ApJ, 665, 1489
Kennicutt, Jr. R. C., 1998, ApJ, 498, 541
Kimm T. et al., 2009, MNRAS, 394, 1131
Kimm T., Yi S. K., Khochfar S., 2011, ApJ, 729, 11
Kitzbichler M. G., White S. D. M., 2006, MNRAS, 366, 858
Knobel C. et al., 2012, ApJ, 753, 121
Kormendy J., Kennicutt, Jr. R. C., 2004, ARA&A, 42, 603
Larson R. B., Tinsley B. M., Caldwell C. N., 1980, ApJ, 237, 692
Lidman C. et al., 2013, MNRAS, 433, 825
Lin L. et al., 2010, ApJ, 718, 1158
Lintott C. J. et al., 2009, MNRAS, 399, 129
Liu F. S., Mao S., Deng Z. G., Xia X. Y., Wen Z. L., 2009, MNRAS, 396, 2003
Magorrian J. et al., 1998, AJ, 115, 2285
Maier C. et al., 2016, A&A, 590, A108

Marconi A., Hunt L. K., 2003, ApJ, 589, L21
Martig M., Bournaud F., Croton D. J., Dekel A., Teyssier R., 2012, ApJ, 756, 26
Martin D. C. et al., 2005, ApJ, 619, L1
Martin D. C. et al., 2007, ApJS, 173, 342
Masters K. L. et al., 2011, MNRAS, 411, 2026
McIntosh D. H., Guo Y., Hertzberg J., Katz N., Mo H. J., van den Bosch F. C., Yang X., 2008, MNRAS, 388, 1537
Merchán M., Zandivarez A., 2002, MNRAS, 335, 216
Merchán M. E., Zandivarez A., 2005, ApJ, 630, 759
Merritt D., Ferrarese L., 2001, MNRAS, 320, L30
Mihos J. C., Hernquist L., 1994, ApJ, 431, L9
Mihos J. C., Hernquist L., 1996, ApJ, 464, 641
Miller C. J. et al., 2005, AJ, 130, 968
Moore B., Katz N., Lake G., Dressler A., Oemler A., 1996, Nature, 379, 613616
Muñoz-Cuartas J. C., Müller V., 2012, MNRAS, 423, 1583
Muldrew S. I. et al., 2012, MNRAS, 419, 2670
Muzzin A. et al., 2012, ApJ, 746, 188
Nair P. B., Abraham R. G., 2010, ApJL, 714, L260L264
Navarro J. F., Frenk C. S., White S. D. M., 1995, MNRAS, 275, 56
Noble A. G., Webb T. M. A., Yee H. K. C., Muzzin A., Wilson G., van der Burg R. F. J., Balogh M. L., Shupe D. L., 2016, ApJ, 816, 48
Noeske K. G. et al., 2007, ApJ, 660, L43
Noguchi M., 1988, A&A, 203, 259
Nulsen P. E. J., 1982, MNRAS, 198, 1007
Oh K., Sarzi M., Schawinski K., Yi S. K., 2011, ApJS, 195, 13
Oman K. A., Hudson M. J., 2016, MNRAS, 463, 3083
Paccagnella A. et al., 2016, ApJ, 816, L25
Padmanabhan N. et al., 2008, ApJ, 674, 1217
Peng C. Y., 2007, ApJ, 671, 1098
Peng Y., Maiolino R., Cochrane R., 2015, Nature, 521, 192
Peng Y.-j. et al., 2010, ApJ, 721, 193
Peng Y.-j., Lilly S. J., Renzini A., Carollo M., 2012, ApJ, 757, 4
Phillips J. I., Wheeler C., Cooper M. C., Boylan-Kolchin M., Bullock J. S., Tollerud E., 2015, MNRAS, 447, 698
Pimbblet K. A., 2011, MNRAS, 411, 2637
Pimbblet K. A., Smail I., Kodama T., Couch W. J., Edge A. C., Zabludoff A. I., O'Hely E., 2002, MNRAS, 331, 333
Poggianti B. M., Smail I., Dressler A., Couch W. J., Barger A. J., Butcher H., Ellis R. S., Oemler, Jr. A., 1999, ApJ, 518, 576
Ponman T. J., Allan D. J., Jones L. R., Merrifield M., McHardy I. M., Lehto H. J., Luppino G. A., 1994, Nature, 369, 462
Pontzen A., Tremmel M., Roth N., Peiris H. V., Saintonge A., Volonteri M., Quinn T., Governato F., 2016, ArXiv e-prints, 1607.02507
Postman M., 2002, in Astronomical Society of the Pacific Conference Series, Vol. 268, Tracing Cosmic Evolution with Galaxy Clusters, Borgani S., Mezzetti M., Valdarnini R., eds., p. 3
Postman M. et al., 2005, ApJ, 623, 721
Roberts I. D., Parker L. C., Karunakaran A., 2016, MNRAS, 455, 3628
Robotham A. S. G. et al., 2011, MNRAS, 416, 2640
Sanders D. B., Soifer B. T., Elias J. H., Madore B. F., Matthews K., Neugebauer G., Scoville N. Z., 1988, ApJ, 325, 74
Schawinski K. et al., 2014, MNRAS, 440, 889
Schawinski K. et al., 2010, ApJ, 711, 284
Schmidt M., 1959, ApJ, 129, 243
Sheth K., Vogel S. N., Regan M. W., Thornley M. D., Teuben P. J., 2005, ApJ, 632, 217
Shimizu M., Kitayama T., Sasaki S., Suto Y., 2003, ApJ, 590, 197
Silk J., Rees M. J., 1998, A&A, 331, L1
Skibba R. A. et al., 2012, MNRAS, 423, 1485
Smail I., Dressler A., Couch W. J., Ellis R. S., Oemler, Jr. A., Butcher H., Sharples R. M., 1997, ApJS, 110, 213
Smethurst R. J. et al., 2016, MNRAS, 463, 2986
Smethurst R. J. et al., 2015, MNRAS, 450, 435
Smith R. et al., 2015, MNRAS, 454, 2502
Snyder G. F., Cox T. J., Hayward C. C., Hernquist L., Jonsson P., 2011, ApJ, 741, 77
Somerville R. S., Hopkins P. F., Cox T. J., Robertson B. E., Hernquist L., 2008, MNRAS, 391, 481
Somerville R. S., Primack J. R., Faber S. M., 2001, MNRAS, 320, 504
Sparre M., Springel V., 2016, ArXiv e-prints, 1610.03850
Springel V., Di Matteo T., Hernquist L., 2005, ApJ, 620, L79
Stoughton C. et al., 2002, AJ, 123, 485
Tago E., Einasto J., Saar E., Tempel E., Einasto M., Vennik J., Müller V., 2008, A&A, 479, 927
Tago E., Saar E., Tempel E., Einasto J., Einasto M., Nurmi P., Heinämäki P., 2010, A&A, 514, A102
Taylor M. B., 2005, in Astronomical Society of the Pacific Conference Series, Vol. 347, Astronomical Data Analysis Software and Systems XIV, Shopbell P., Britton M., Ebert R., eds., p. 29
Tempel E. et al., 2014, A&A, 566, A1
Tinker J., Wetzel A., Conroy C., 2011, ArXiv e-prints, 1107.5046
Tonini C., Mutch S. J., Croton D. J., Wyithe J. S. B., 2016, MNRAS, 459, 4109
Toomre A., 1977, in Evolution of Galaxies and Stellar Populations, B. M. Tinsley & R. B. G. Larson D. Campbell, ed., p. 401
Toomre A., Toomre J., 1972, ApJ, 178, 623
Treister E., Schawinski K., Urry C. M., Simmons B. D., 2012, ApJ, 758, L39
Tucker D. L. et al., 2000, ApJS, 130, 237
van de Voort F., Bahé Y. M., Bower R. G., Correa C. A., Crain R. A., Schaye J., Theuns T., 2016, ArXiv e-prints, 1611.03870
Walker I. R., Mihos J. C., Hernquist L., 1996, ApJ, 460, 121
Wang W., Sales L. V., Henriques B. M. B., White S. D. M., 2014, MNRAS, 442, 1363
Weiner B. J. et al., 2006, ApJ, 653, 1049
Weinmann S. M., van den Bosch F. C., Yang X., Mo H. J., 2006, MNRAS, 366, 2
Wetzel A. R., Tinker J. L., Conroy C., van den Bosch F. C., 2013, MNRAS, 432, 336
Whitaker K. E. et al., 2016, ArXiv e-prints, 1607.03107
Willett K. W. et al., 2013, MNRAS, 435, 2835
Woo J., Dekel A., Faber S. M., Koo D. C., 2015, MNRAS, 448, 237
Wyder T. K. et al., 2007, ApJS, 173, 293

Yang X., Mo H. J., van den Bosch F. C., Pasquali A., Li C., Barden M., 2007, ApJ, 671, 153
Yesuf H. M., Faber S. M., Trump J. R., Koo D. C., Fang J. J., Liu F. S., Wild V., Hayward C. C., 2014, ApJ, 792, 84
York D. G. et al., 2000, AJ, 120, 1579
Zurita A., Relaño M., Beckman J. E., Knapen J. H., 2004, A&A, 413, 73
Zwicky F., 1938, PASP, 50, 218
Zwicky F., 1952, PASP, 64, 247